

SHERMAN DAM
SEISMIC STABILITY EVALUATION

FEDERAL ENERGY REGULATORY COMMISSION

RECEIVED

JUL - 6 1982

NEW YORK, N. Y.

Submitted to

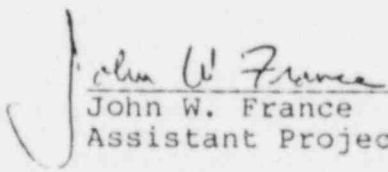
New England Power Company
Westborough, Massachusetts

Prepared by

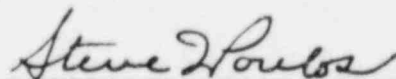
Geotechnical Engineers Inc.
1017 Main Street
Winchester, Massachusetts
(617) 719-1625

Project 82917

April 9, 1982


John W. France

Assistant Project Manager


Steve J. Poulos

Principal

TABLE OF CONTENTS

	<u>Page No.</u>
LIST OF TABLES	
LIST OF FIGURES	
LIST OF APPENDICES	
1. INTRODUCTION	1
1.1 Purpose	1
1.2 Technical Approach	1
1.3 Background	1
1.4 Sources of Data	2
2. SUMMARY AND CONCLUSIONS	3
3. CROSS SECTION OF SHERMAN DAM	4
4. SEISMIC STABILITY	6
4.1 General	6
4.2 Strength Parameters For Flow Slide Stability Analysis	6
4.2.1 General	6
4.2.2 Hydraulic Core	7
4.2.3 Dumped Shell	7
4.2.4 Rolled Shell	8
4.2.5 Glacial Till Foundation Soil	8
4.3 Results of Flow Slide Stability Analyses	9
4.3.1 Method of Analysis	9
4.3.2 Results For Downstream Slope	9
4.3.3 Results For Upstream Slope	9
4.4 Conclusions	10
5. EVALUATION OF DEFORMATIONS DURING SEISMIC LOADING	11
5.1 General	11
5.2 Input Earthquake Motion	11
5.3 Computation of Earthquake Shear Stresses	12
5.4 Computations of Strains and Deformations	12
5.5 Conclusions	14
6. LIST OF REFERENCES	15
TABLE	
FIGURES	
APPENDICES	

LIST OF TABLES

Table 1 - Calculated Accumulated Deformations of Sherman
Dam During Seismic Loading

LIST OF FIGURES

- Fig. 1 - Location Map
- Fig. 2 - Interpretive Cross-Section - Sherman Dam Sta 16+00
- Fig. 3 - Idealized Cross-Section Used For Seismic Stability Evaluation
- Fig. 4 - Summary of Flow Slide Stability Analysis of Downstream Slope
- Fig. 5 - Summary of Flow Slide Stability Analysis of Upstream Slope
- Fig. 6 - Earthquake Response Spectra
- Fig. 7 - Finite Element Mesh Highest Section Sherman Dam
- Fig. 8 - Earthquake Shear Stresses Vs Depth At Highest Section
- Fig. 9 - Equivalent Number of Uniform Stress Cycles
- Fig. 10 - Shear Strain Vs Depth At Highest Section

LIST OF APPENDICES

- APPENDIX A - Selection of Strength Parameters For
Flow Slide Stability Analyses
- APPENDIX B - Determination of Undrained Steady State
Shear Strengths For Hydraulic Core of
Sherman Dam
- APPENDIX C - Some Details of the Evaluation of Strains
and Deformations During Seismic Loading

1. INTRODUCTION

1.1 Purpose

The purpose of this report is to present the results of a preliminary seismic stability evaluation of Sherman Dam performed by Geotechnical Engineers Inc. (GEI).

1.2 Technical Approach

The analysis consisted of two parts:

- a. Evaluation of the overall stability of the dam under seismic loading.
- b. Estimation of the movements of the dam that would be caused by seismic loading.

1.3 Background

Sherman Dam is owned by New England Power Company and is located near Monroe Bridge, MA, as shown in Fig. 1. The Yankee Rowe Nuclear Plant is immediately adjacent to the left abutment (looking downstream).

New England Power Company engaged C. T. Main, Inc. to perform an inspection of Sherman Dam in accordance with Federal Energy Regulatory Commission (FERC) regulations. As part of the inspection program, GEI was engaged to carry out a preliminary field and laboratory program, as requested by C. T. Main, Inc., and to perform a seismic stability analysis.

The field exploration program consisted of six borings in the dam and two borings in the left abutment. Also 19 piezometers were installed. The principal intent of this program was to establish the cross section of the dam at one (the highest) section and to recover samples of the core and shell for laboratory testing. All data needed for analysis, but not obtained from this preliminary program, were to be estimated based on data available for Harriman Dam or based on past experience.

In particular, the dynamic shear moduli and damping ratios in the core and shell of Sherman Dam were not measured. Also, the shear strength of the glacial till shell was not measured because the material was too dense and/or too gravelly to yield satisfactory undisturbed samples. However, these properties were measured for Harriman Dam. Therefore, for the analysis of Sherman Dam, conservative values of the shear strength of the glacial till in the shell and the shear moduli and damping ratios

in both the core and shell were estimated based on comparisons with the data from Harriman Dam. Also, a sensitivity analysis was made to evaluate the effect on the results of reasonable variations in the shear moduli and damping ratios of the core.

1.4 Sources of Data

For Sherman Dam, summaries of construction records and geotechnical data from field and laboratory investigations are presented in two reports, which are available separately, namely Main (1973)* and GEI (1982a). Geotechnical data from field and laboratory investigations of Harriman Dam are presented in three reports, which are available separately, namely GEI (1981a), GEI (1981b), and GEI (1981c).

Earthquake acceleration spectra used for the seismic analysis were taken from Yankee Atomic Electric Co. (1981).

*See List of References in Section 6 of this report.

2. SUMMARY AND CONCLUSIONS

The preliminary seismic stability analyses were performed for the maximum-height cross section of Sherman Dam.

The minimum factor of safety of the downstream slope is 1.3 and of the upstream slope is 2.0 against a flow slide triggered by an earthquake. For this condition, a factor of safety of 1.1 is adequate. For the analyses it was assumed that the core liquefied and that the shell had reached its minimum, or residual strength. The peak strength of the shell was not used.

The deformations expected for two levels of earthquake motion were estimated using finite element analyses. The earthquake assumptions and the results are:

Earthquake spectrum	Yankee Composite	NRC
Peak ground acceleration	0.1 g	0.2 g
Probability of being equaled or exceeded in a given year	10^{-3}	10^{-4}
Calculated crest settlement	0.7 ft	1.3 ft
Calculated horizontal movement:		
Upstream slope (midpoint)	0.4 ft	1.1 ft
Downstream slope (midpoint)	0.3 ft	0.8 ft

Deformations of these magnitudes would not be expected to impair the overall integrity of Sherman Dam, particularly since the minimum freeboard of the dam is 24 ft.

The analyses described above were based on data obtained in the preliminary field and laboratory program for Sherman Dam (GEI, 1982a) and on properties selected based on comparison with Harriman Dam, as described in Section 1.3 and in the text of this report.

3. CROSS SECTION OF SHERMAN DAM

The seismic stability evaluation was performed for the maximum-height cross section of Sherman Dam, as shown in Fig. 2. The interpretive cross section in Fig. 2 is reproduced from GEI (1982a) and was based on construction records and on the results of test borings performed between June and September 1982.

Sherman Dam was constructed by a modified hydraulic fill method. Glacial till was dumped to form berms on the upstream and downstream sides of the dam. The inside slopes of the berms were washed with water and the fines were allowed to settle out of the resulting puddle to form the dam core. New upstream and downstream berms of dumped glacial till were then constructed to higher elevations and the inside slopes were washed to raise the core. Railroad tracks supported by wooden trestles were constructed on top of each berm so that the soil for the next berm could be brought in by train. The wooden trestles were buried in the later berms. The process of constructing berms and washing the inside slopes was repeated until the core had been constructed to the desired elevation. Glacial till was then dumped into place above the core to raise the crest of the dam to the design elevation.

Based on the construction records, typical berm and trestle locations are shown in Fig. 2. The "beach lines" shown in Fig. 2 delineate the edges of the central puddles created by the washing process. The soil between the beach lines was deposited through water after being washed out of the dumped glacial till berms. On the upstream and downstream sides of the beach lines, a "shore" was formed where coarser particles settled out from the flowing water. The "80% minus #100 sieve lines" shown in Fig. 2 were determined during construction. Inside these lines, all soil samples tested during construction had greater than 80% by weight of the particles finer than the #100 sieve size.

Based on this construction history of the dam three separate zones would be expected: (1) a dumped shell, (2) a core (inside the 80% minus #100 sieve lines) and (3) an intermediate zone (the washed material between the dumped shell and the core).

The results of Borings 102 and 107 did indicate a boundary at approximately the location of the 80% minus #100 sieve lines. The soil samples inside this zone were predominantly stratified fine sand and silt, and for analysis purposes, this zone has been called the hydraulic core, as shown in Fig. 2. However, based on visual descriptions, grain-size distributions and blowcounts, the dumped shell and the intermediate zone of Sherman Dam could not

be distinguished from each other (GEI, 1982a). For analysis purposes, these two zones were considered to be the same soil and are referred to in this report as the "dumped shell" material.

In 1964, Sherman Dam was raised by constructing a new section, composed of glacial till borrow, over the crest and downstream slope. This section was compacted mechanically with rollers and is designated as "rolled shell" in Fig. 2.

The simplified cross section used for the seismic stability evaluation consists of three zones - the core, the dumped shell and the rolled shell, as shown in Fig. 3.

4. SEISMIC STABILITY

4.1 General

The first step in the seismic analysis of Sherman Dam is to estimate the factor of safety against a flow slide resulting from liquefaction of the soils comprising the dam.

Liquefaction occurs when a mass of soil loses a large percentage of its shear strength when subjected to undrained monotonic, cyclic or shock loading, and deforms continuously until the shear stresses acting on the mass are as low as the reduced shear strength, which is referred to as the undrained steady-state shear strength.

The loss in shear strength results from a disturbance (e.g., an earthquake) which converts the mass from a drained condition, in which it can sustain the in situ shear stresses, to an essentially undrained condition in which the shear resistance of the mass is lower than the imposed shear stresses.

A flow slide results if liquefaction occurs in a sufficiently large mass of the soil.

The procedure used for analyzing the potential for a flow slide failure is as follows (GEI, 1982b):

- a. Calculate the static driving shear stresses, τ_d , in various zones of the dam and compare with the undrained steady-state shear strengths, S_{US} .
- b. Perform stability analyses using (1) the undrained steady state shear strength, S_{US} , in zones where τ_d is greater than S_{US} (i.e., where liquefaction is likely) and (2) appropriate undrained or drained strengths (depending on gradation of the soil) in zones where τ_d is less than S_{US} (i.e., liquefaction is not possible).
- c. Calculate the factors of safety from the stability analyses.

4.2 Strength Parameters For Flow-Slide Stability Analysis

4.2.1 General

This section contains a summary of our selections for strength parameters for the flow-slide stability analysis.

A more detailed discussion of the selections is presented in Appendix A.

4.2.2 Hydraulic Core

Estimated static driving shear stresses, τ_d , in the hydraulic core were calculated from trial slip circle stability analyses. Undrained steady-state shear strengths, S_{US} , were estimated from the results of laboratory triaxial tests. For most of the core, the estimated driving shear stresses were higher than the estimated steady-state strengths. Therefore, most of the core would be susceptible to liquefaction. Hence, we assumed that the core would liquefy, and based on the triaxial test data, we selected an undrained steady-state shear strength (after liquefaction), $S_{US} = 700$ psf. The selection of this value of S_{US} is explained in more detail in Appendix A.

4.2.3 Dumped Shell

In this analysis, the term "dumped shell" will refer to both the section of the shell that was dumped in place during construction and the intermediate zone adjacent to the hydraulic core, because samples from both of these zones had similar physical composition and similar blowcounts (GEI, 1982a).

No borings were performed in the upstream shell of Sherman Dam (GEI, 1982a). Hence, no samples of the upstream shell were obtained. Construction records show that the upstream and downstream shells were constructed from the same borrow soils and in the same manner. So, in this analysis, the same stress-deformation properties were assumed for the upstream and the downstream shells of Sherman Dam.

In the borings in the downstream shell, we were not successful in obtaining undisturbed samples, despite ten attempts during the field exploration program (GEI, 1982a). Because of the lack of undisturbed samples, we estimated the stress-deformation properties of the Sherman Dam shell based on comparisons with the Harriman Dam shell.

The visual descriptions, the grain-size distributions, the method of placement of the materials, and the blowcounts for the Sherman Dam shell are essentially the same as those for the Harriman Dam shell (GEI, 1982a). Therefore, we used results of tests on undisturbed samples of the Harriman Dam shell to estimate the shear strengths of the Sherman Dam shell.

The undrained steady-state shear strength, S_{us} , of the Harriman Dam shell material was estimated from the results of five tests on undisturbed samples (CEI, 1981b; GEI, 1981c). The undrained steady-state shear strength, S_{us} , is the minimum shear strength during undrained unidirectional shear of a soil, and the strength is reduced to this value only after very large shear deformation (GEI, 1982b).

Based on the data from Harriman Dam, we selected an undrained steady-state shear strength of $S_{us} = 2,000$ psf for the Sherman Dam shell for use in the flow slide analyses. The selection of this value of S_{us} is explained in more detail in Appendix A. This is a conservative estimate of the strength of the Sherman Dam shell for three reasons. First, the undrained steady-state shear strength is the minimum strength during undrained shear. Second, in the Harriman Dam shell, we attempted to take 93 tube samples but obtained only 45 samples with greater than 7 in. of recovery. Only 27 of those samples were acceptable for laboratory testing. Hence, the tube samples of Harriman Dam that were tested in the laboratory probably represent the looser and less gravelly zones of the shell, and the average strength of the shell probably is higher than that obtained from the tube samples. Third, in the Sherman Dam shell we attempted to take ten tube samples and obtained no samples with greater than 7 in. of recovery. This suggests that the Sherman Dam shell may be, on average, denser and/or more gravelly, and hence stronger, than the Harriman Dam shell.

4.2.4 Rolled Shell

Drained strengths corresponding to a friction angle $\phi = 45^\circ$ and zero cohesion were selected for the unsaturated rolled shell, based on tests on similar soils from Harriman Dam.

Drained strength is appropriate for the rolled shell because it is above the water level, as illustrated in Fig. 3.

4.2.5 Glacial Till Foundation Soil

Drained strengths corresponding to a friction angle $\phi = 40^\circ$ and zero cohesion were selected for the glacial till beneath the dam. No test data were available for the till. This value is a conservative estimate of the friction angle of the undisturbed till.

The till is dense enough that it is dilative and, hence, its undrained strength would be greater than its drained strength. However, negative pore water pressures are required to mobilize this higher undrained strength. These negative pressures should not be relied upon in the stability analysis. Therefore, the drained strength, which corresponds to zero induced pore pressure, is a reasonable strength to use in the undrained stability analyses for the portion of the trial surface in the glacial till foundation.

4.3 Results of Flow-Slide Stability Analyses

4.3.1 Method of Analysis

The flow-slide stability of the upstream and downstream slopes during and after an earthquake was evaluated using both circular-arc-slip-surface and sliding-wedge analyses.

The circular-arc-slip-surface analyses were performed using the computer program STABL2 (Siegel, 1975 and Boutrup, 1978). The program uses the modified Bishop method (a limit equilibrium method of finite slices) and includes critical-surface searching options.

The sliding-wedge analyses were performed by hand.

The reservoir elevation used in the stability analysis was the maximum operating pool at El 1000 (NEPCo datum). Seepage pressures within the dam were estimated from the piezometer readings taken when the pool was at El 999.

Analyses were performed for both the downstream and upstream slopes using the strength parameters described in Section 4.2.

4.3.2 Results For Downstream Slope

The results of the stability analyses of the downstream slope are summarized in Fig. 4. The minimum computed factor of safety was 1.3. As shown in Fig. 4, the critical surface was a sliding wedge with a horizontal surface at the base of the dam.

4.3.3 Results For Upstream Slope

The results of the stability analyses of the upstream slope are summarized in Fig. 5. The minimum computed factor of safety was 2.0. As shown in Fig. 5, the critical surface

was a circular arc which passed through the core. The upstream slope would be expected to be less critical during seismic loading, since the upstream slope is flatter.

4.4 Conclusions

The minimum computed factor of safety against a flow slide is 1.3. For this condition, a factor of safety of 1.1 would be adequate. As dissipation of excess pore-water pressures occurs after the earthquake, the drained shear conditions existing prior to the earthquake will be re-established and the factors of safety for static load conditions will become applicable again.

The strengths used to compute the factor of safety of 1.3 were the undrained steady-state strengths in the core and in the shell. This strength is the minimum or "residual" strength rather than the peak strength, which is often used in analyses of this type.

We conclude that a flow slide cannot occur even if the core liquefies.

5. EVALUATION OF DEFORMATIONS DURING SEISMIC LOADING

5.1 General

Even though a dam may have sufficient resistance against an earthquake-induced flow slide (as concluded for Sherman Dam in Section 4), the dam will still undergo some deformations due to the shear stresses and strains resulting from an earthquake.

The following procedure was used to evaluate the deformations during seismic loading:

1. Select the design earthquake input motion.
2. Using a two-dimensional finite-element model, calculate the shear stresses in the dam during the seismic loading.
3. Using laboratory cyclic load test data, estimate the strains that will result in various sections of the dam as a result of the shear stresses calculated in (2), above.
4. Integrate the strains calculated in (3), above, to estimate deformations of the dam.

The analysis is summarized in this section and some of the details are discussed in Appendix C.

5.2 Input Earthquake Motion

Two input earthquake motions were used in the analysis, each conforming to one of the following earthquake spectra:

1. The Yankee composite spectrum (Yankee, 1981).
2. The NRC response spectrum (NRC, 1981).

The Yankee composite spectrum has an estimated 10^{-3} probability of being exceeded in any given year (Yankee, 1981) and, in our opinion, is a reasonably conservative design earthquake. The more conservative NRC response spectrum has an estimated 10^{-4} probability of being exceeded in any given year and was included for comparison purposes.

Input earthquake motions consisting of the Housner earthquake record (an artificial record) scaled to 0.1g and 0.2g maximum ground accelerations were used in the analysis to represent

the Yankee and NRC spectra, respectively. Conformance between the scaled earthquake records and the Yankee and NRC spectra is illustrated in Fig. 6.

5.3 Computation of Earthquake Shear Stresses

Earthquake-induced shear stresses in Sherman Dam were estimated using the two-dimensional finite-element program FLUSH (Lysmer *et al.*, 1975), with the finite-element mesh shown in Fig. 7. For this analysis, the required dynamic soil properties (modulus and damping factors) were selected based on comparisons to laboratory test data from samples of Harriman Dam, as discussed in Appendix C. The input earthquake motion was applied to the base of the dam as a horizontal motion.

Several finite-element analyses were performed to evaluate the sensitivity of the analysis to the configuration of the core and to the input moduli for the core. The analysis was relatively insensitive to reasonable variations in these parameters, as discussed in Appendix C. Hence, only the results for the core configuration and soil properties judged to be most likely are presented in this section.

In Fig. 8, the resulting values of maximum earthquake shear stress, for both the 0.1g and the 0.2g earthquakes, are plotted versus depth for vertical soil columns at three locations: (1) the midpoint of the downstream slope, (2) the centerline of the core, and (3) the midpoint of the upstream slope. Note that these are the maximum earthquake shear stresses that will occur for each element at some time during the earthquake and do not necessarily occur simultaneously.

5.4 Computations of Strains and Deformations

We estimated accumulated strains due to earthquake loading for individual finite elements by the following procedure:

1. Calculate cyclic triaxial test stresses comparable to the earthquake shear stresses from the finite element analysis.
2. From laboratory data, estimate the amount of strain that would have accumulated in a cyclic triaxial test performed with these comparable stresses.
3. Assume that the accumulated strain estimated in Step (2) occurs in the element in the field.

4. Correct the calculated stresses and strains for any incompatibility that results from the computations.

The maximum earthquake shear stresses, from the finite element analysis, τ_{max} , shown in Fig. 8, occur only once during the duration of the earthquake. To compare these shear stresses to the uniform cyclic shear stresses used in laboratory cyclic triaxial test, equivalent average uniform cyclic shear stresses, τ_{avg} , are computed using the relationship $\tau_{avg} = 0.65\tau_{max}$. These shear stresses are then used to calculate the stress ratios $\tau_{avg}/\bar{\sigma}_v$, where $\bar{\sigma}_v$ is the effective vertical stress prior to the earthquake. These stress ratios are used to determine comparable cyclic triaxial test conditions.

From laboratory cyclic triaxial test data, plots of the stress ratio $\tau_{fy}/\bar{\sigma}_{fc}$ vs accumulated shear strain for seven cycles of load were developed, where τ_{fy} is the cyclic shear stress on the potential failure plane and $\bar{\sigma}_{fc}$ is the effective normal consolidation stress on the same plane. Separate plots were constructed for the core and for the shell. The plot for the core was based on cyclic triaxial tests on tube samples from the core of Sherman Dam. Because no cyclic triaxial test data are available for the shell of Sherman Dam, the plot for the shell was based on cyclic triaxial tests on tube samples from the shell of Harriman Dam. The use of the Harriman Dam data was based on the inference that the stress-deformation properties of the shells of the two dams are similar because of the similarity of the physical composition, method of placement, and the blowcounts (see Section 4.2.3). The development of these plots is discussed in Appendix C.

The selection of seven cycles of load was based on a conservative interpretation of a published relationship between earthquake magnitude and equivalent number of cycles at $0.65\tau_{max}$ (see Fig. 9). A maximum expected earthquake magnitude of 6.0 was used, based on information in Yankee, 1981.

To estimate accumulated shear strains for the individual elements in the dam the appropriate plots of stress ratio $\tau_{fy}/\bar{\sigma}_{fc}$ vs accumulated shear strain were entered with $\tau_{fy}/\bar{\sigma}_{fc} = \tau_{avg}/\bar{\sigma}_v$ (i.e., stress ratio in the cyclic triaxial test comparable to stress ratio from the finite element analysis).

Because of the large difference between the deformabilities of the hydraulic core and of the dumped shell, the method described above leads to the case where the accumulated strains in elements of the core are significantly higher than the accumulated strains in immediately adjacent elements of the shell. In

reality this incompatibility of accumulated strains in adjacent elements cannot occur and will be prevented by load transfer from the more deformable core to the less deformable shell. In this analysis, when the calculated strains were incompatible, an estimate of the load transfer and of the resulting compatible strains and stresses was made by hand computation, as described in Appendix C.

In Fig. 10, the calculated accumulated shear strains (with compatibility corrections, where required) for both the 0.1g and the 0.2g earthquake are plotted versus depth for the same three vertical soil columns used in Fig. 8. For the 0.1g earthquake, all of the calculated strains are less than 1.5 percent, and for the 0.2g earthquake the strains are generally less than 3 percent.

Calculated accumulated horizontal displacements at the midpoints of the upstream and downstream slopes were determined by integrating the accumulated strains in Fig. 10, and the results are summarized in Table 1.

A calculated accumulated crest settlement was determined by integrating the accumulated strains in Fig. 10 for the vertical column through the crest, assuming that these strains represent maximum shear strains inclined at an angle of 45° from the vertical with Poisson's ratio, $\nu = 0.5$ (i.e., undrained conditions), and the results are presented in Table 1. (Use of any other orientation for the assumed direction of the maximum shear strains would yield a smaller calculated crest settlement.)

5.5 Conclusions

The estimated horizontal deformation and crest settlements resulting from either the 0.1g or the 0.2g earthquake are presented in Table 1. The maximum estimated movement in any direction is 1.3 ft. Such movement should have a minor effect because:

1. The freeboard of the dam is about 24 ft, even at the maximum reservoir operating level of El 1000.
2. Although significant transverse cracking of the dam is not expected as a result of the estimated deformations, the widely graded dumped shell materials would be self-healing, even if transverse cracking should occur.

It is concluded that Sherman Dam has adequate seismic resistance for either the 0.1 g or 0.2 g earthquake.

6. LIST OF REFERENCES

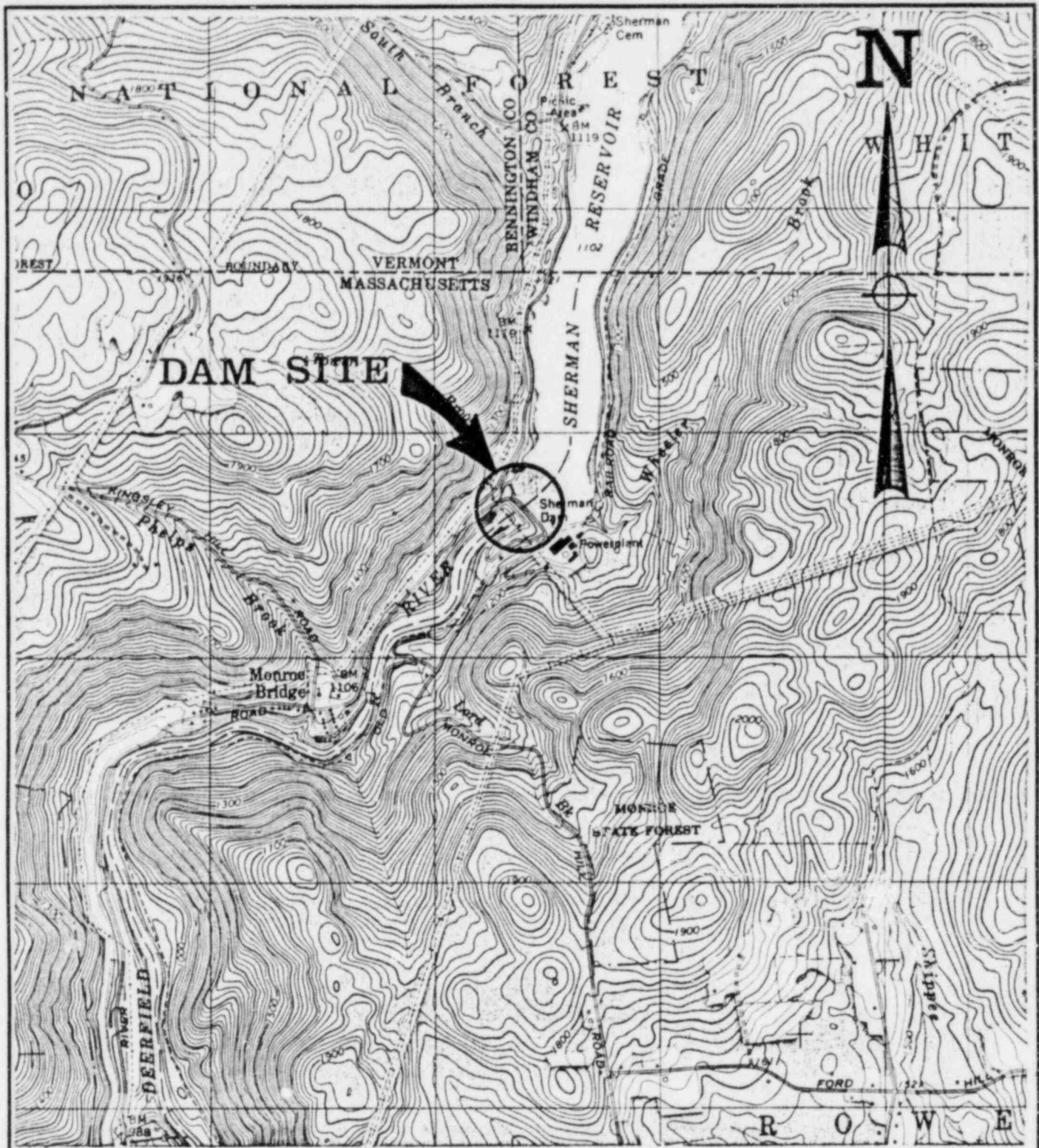
1. Castro, G. (1975), "Liquefaction and Cyclic Mobility of Saturated Sands," Journal of the Geotechnical Engineering Division, ASCE, Vol. 101, No. GT6, June 1975, pp. 551-569.
2. C. T. Main, Inc. (1973), "Second Inspection Report of the New England Power Company Deerfield River Project," submitted to Federal Energy Regulatory Commission.
3. Geotechnical Engineers Inc. (1981a), "Harriman Dam, Summary of Field Investigations and Laboratory Tests for Phases I and II," Project 79646, April 10, 1981.
4. Geotechnical Engineers Inc. (1981b), "Harriman Dam, Summary of Field Investigations and Laboratory Tests for Phase III," Project 81807, August 13, 1981.
5. Geotechnical Engineers Inc. (1981c), "Harriman Dam, Seismic Stability Evaluation," Project 81858, December 23, 1981.
6. Geotechnical Engineers Inc. (1982a), "Sherman Dam, Summary of Field Investigations and Laboratory Tests," Project 81837, January 22, 1982.
7. Geotechnical Engineers Inc. (1982b), "Report on Liquefaction Induced by Cyclic Loading," prepared for the National Science Foundation, NSF Grant No. PFR-7924731, GEI Project 80696, March 1982.
8. Hardin, B. O. and Richart, F. E., Jr. (1963), "Elastic Wave Velocities in Granular Soils," Journal of the Soil Mechanics and Foundation Division, ASCE, Proceedings, Vol. 89, No. SM1, February 1963, pp. 33-65.
9. Kim, T. C. and Novak, M. (1981), "Dynamic Properties of Some Cohesive Soils of Ontario," Canadian Geotechnical Journal, V. 18, pp. 371-389.
10. Lysmer, J.; Udaka, T.; Tsai, C.-F.; and Seed, H. B. (1975), "FLUSH - A Computer Program for Approximate 3-D Analysis of Soil-Structure Interaction Problems," Earthquake Engineering Research Center, University of California, Berkeley, Report No. EERC 75-30, November 1975.
11. Nuclear Regulatory Commission (1981), "Site Specific Ground Response Spectra for SEP Plants Located in Eastern United States," NRC letter to all SEP plant owners, from Mr. Dennis

- M. Crutchfield, Chief, Operating Reactors Branch, Division of Licensing, June 8, 1981.
12. Seed, H. B. (1976), "Evaluation of Soil Liquefaction Effects on Level Ground During Earthquakes," from Liquefaction Problems in Geotechnical Engineering, Specialty Session at ASCE Annual Convention, Philadelphia, Sept. 27-Oct. 1, 1976.
 13. Yankee Atomic Electric Co. (1981), "Seismic Response Spectra for the Yankee Rowe Nuclear Power Station, Rowe, Massachusetts," June 1981.

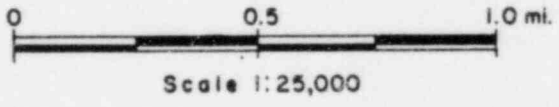
TABLE 1 - CALCULATED ACCUMULATED DEFORMATIONS⁽¹⁾ OF
SHERMAN DAM DURING SEISMIC LOADING


Input Earthquake Motion	Calculated Accumulated Deformations		
	Crest Settlement ⁽²⁾	Horizontal Displacements at Midpoint of Slope ⁽³⁾ , ft	
	ft	Upstream	Downstream
Housner with 0.1g maximum ground acceleration	0.7	0.4	0.3
Housner with 0.2g maximum ground acceleration	1.3	1.1	0.8

- NOTES: (1) Accumulated deformations were calculated for the maximum height cross section of the dam, based on shear stresses from a finite element analysis and stress-deformation properties from laboratory tests (see Section 5 of the text).
- (2) Crest settlement was calculated by integrating estimated shear strains in a vertical soil column through the dam assuming that the shear strains occur on a plane inclined at 45° from the vertical (see Section 5.4 of the text).
- (3) Horizontal displacements were calculated by integrating estimated shear strains in vertical soil columns through the dam (see Section 5.4).



From: Rowe, Massachusetts Quadrangle
USGS Topographic Map



New England Power Company Westborough, Massachusetts	Seismic Stability Evaluation Sherman Dam	LOCATION MAP
 GEOTECHNICAL ENGINEERS INC. WINCHESTER • MASSACHUSETTS	Project 81837	February 5, 1982 Fig. 1

DOCUMENT/ PAGE PULLED

ANO. 8209170055

NO. OF PAGES 1

REASON

PAGE ILLEGIBLE

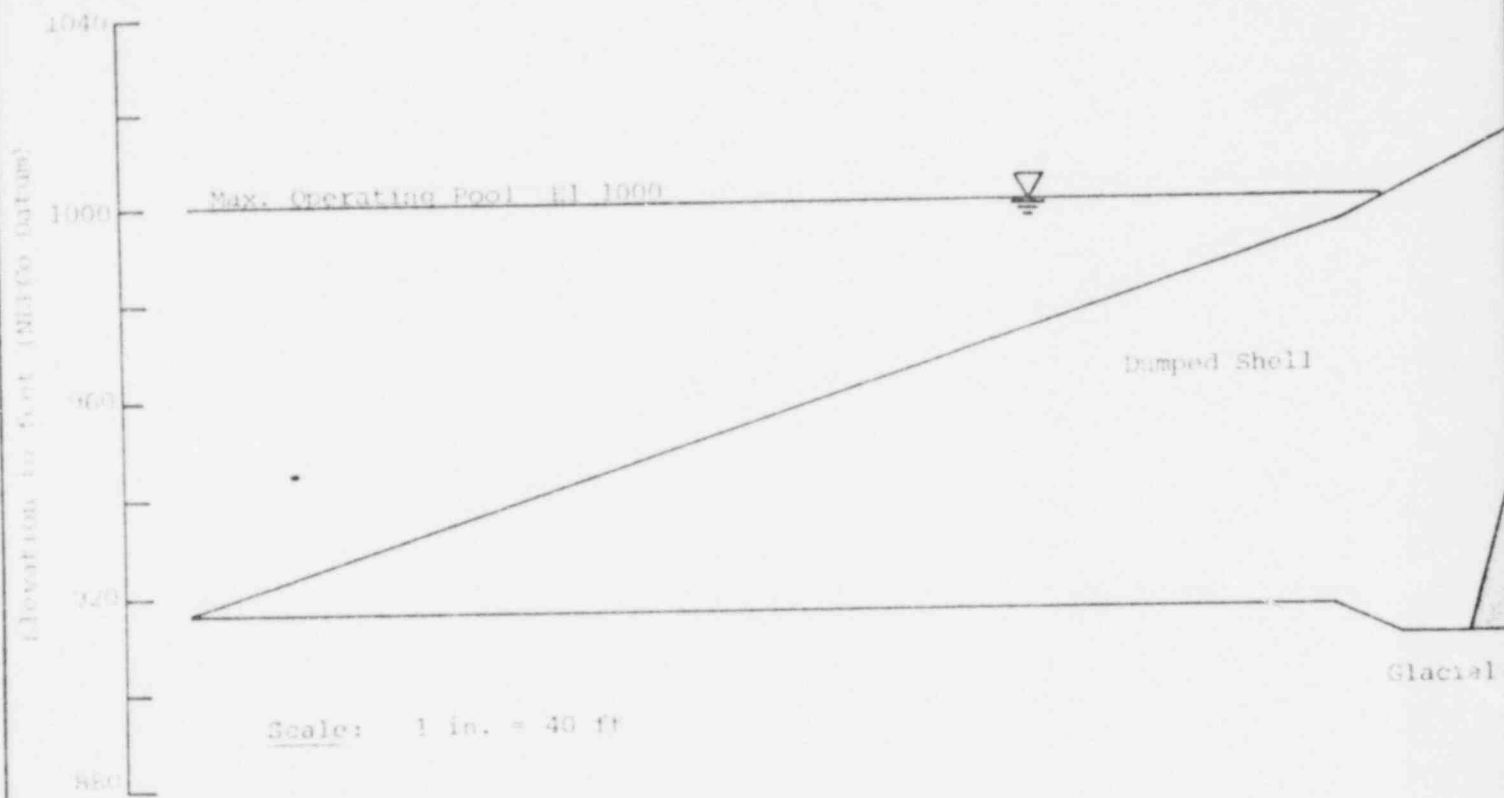
HARD COPY FILED AT. PDR CF
OTHER _____

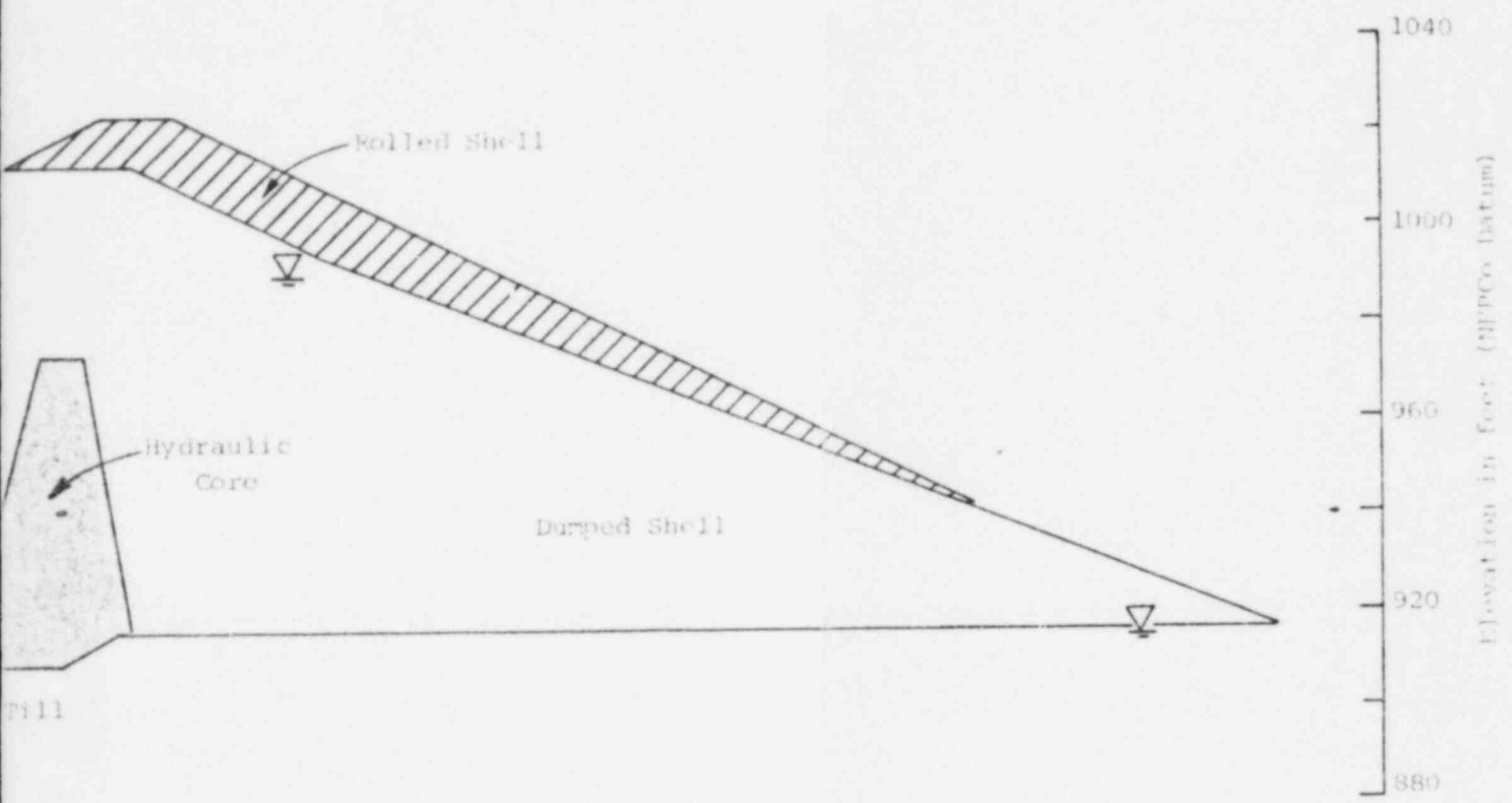
BETTER COPY REQUESTED ON _____


PAGE TOO LARGE TO FILM

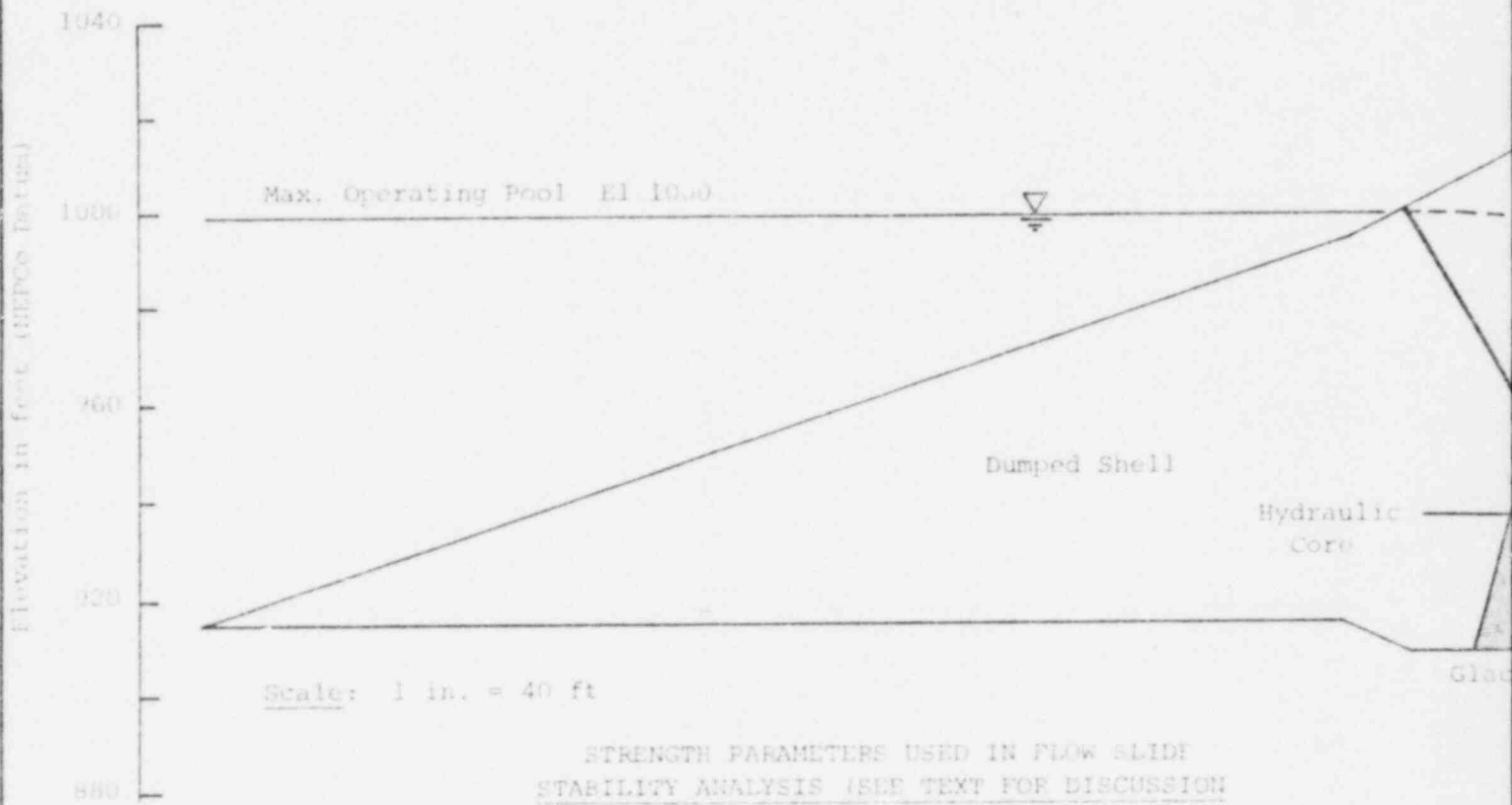
HARD COPY FILED AT. PDR CF
OTHER _____

FILMED ON APERTURE CARD NO 8209170055-01

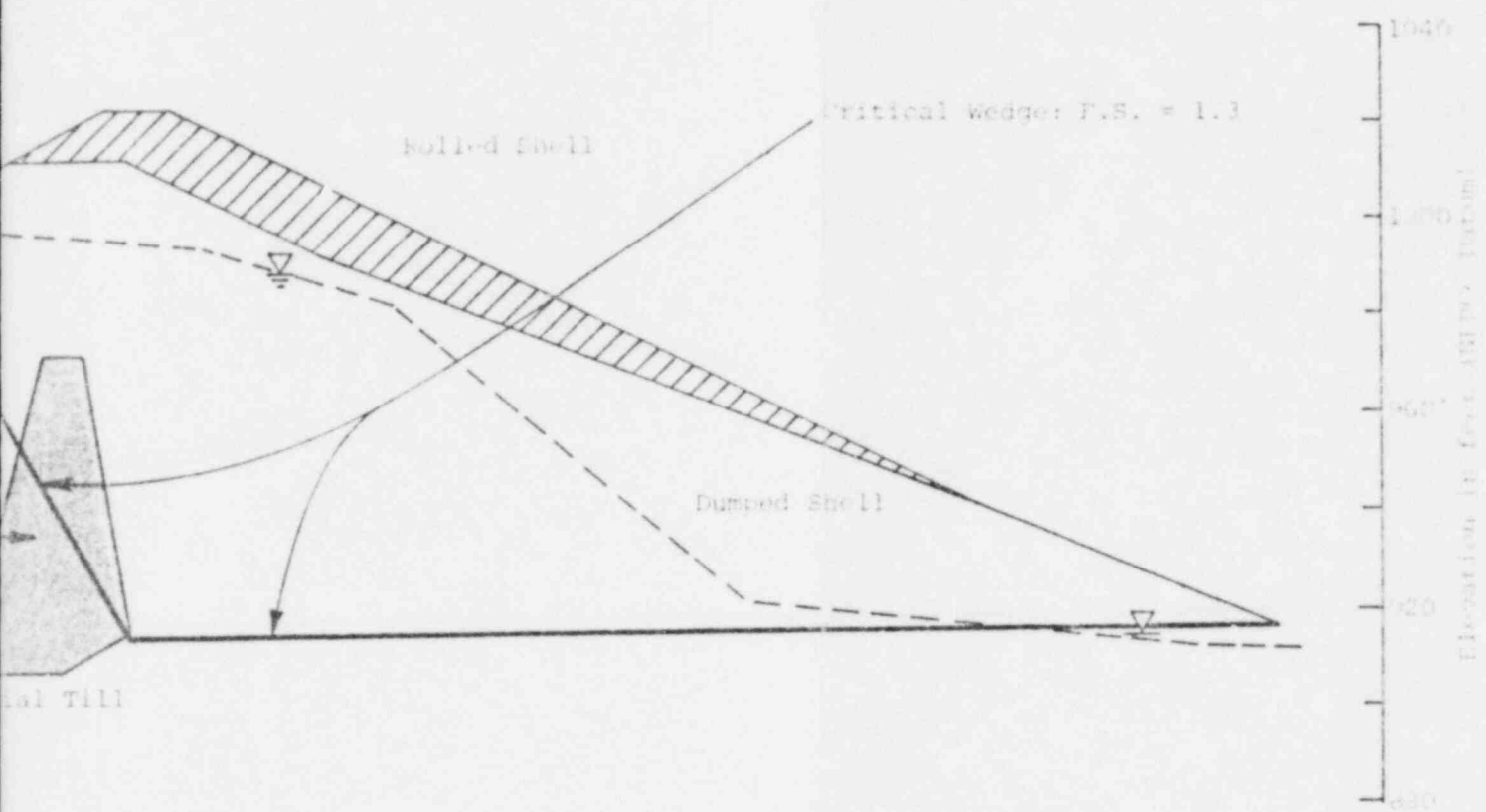





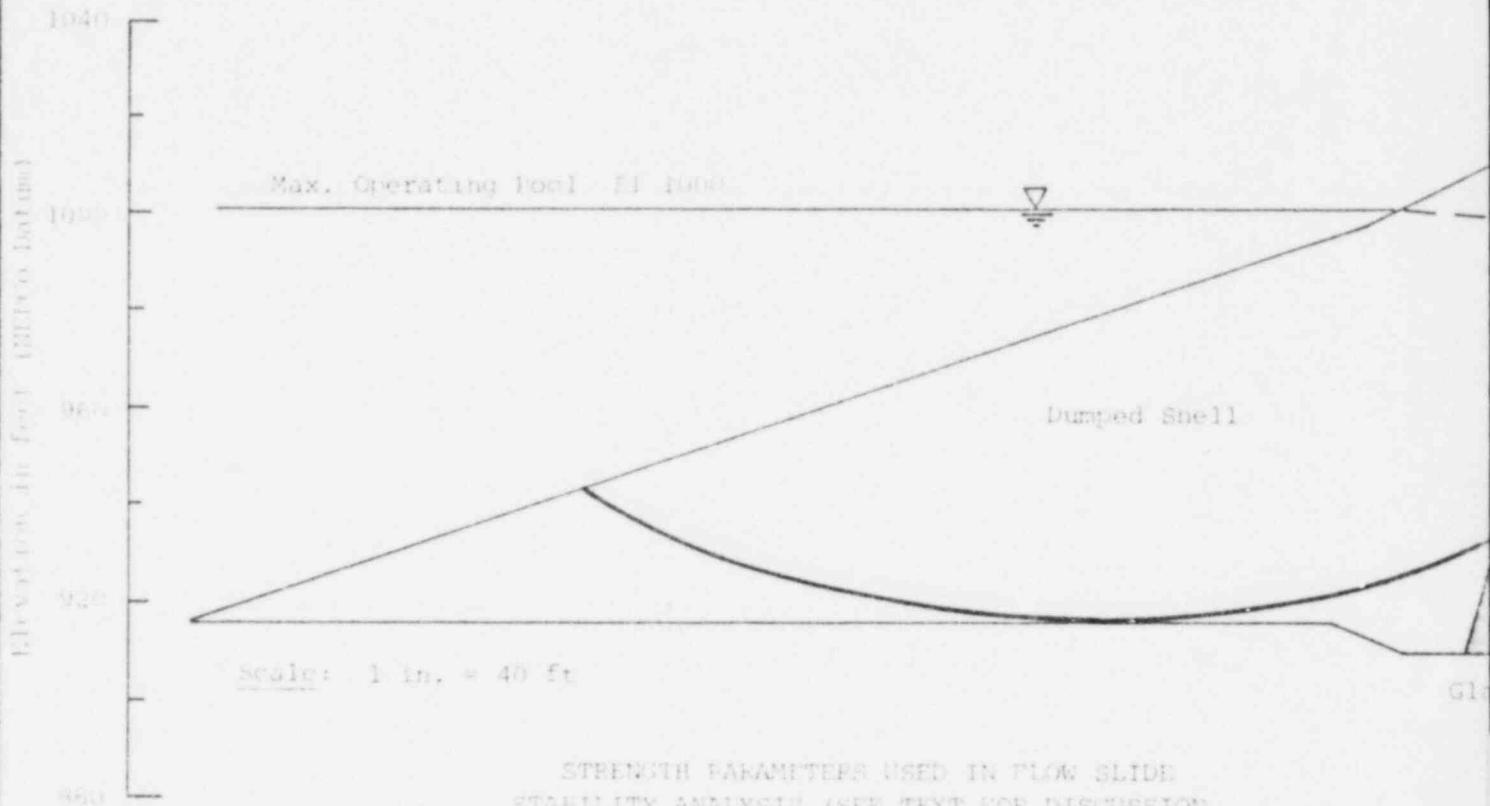
New England Power Company Westborough, Massachusetts	Seismic Stability Evaluation Sherman Dam	IDEALIZED CROSS SECTION USED FOR SEISMIC STABIL- ITY EVALUATION
 GEOTECHNICAL ENGINEERS INC WINCHESTER • MASSACHUSETTS	Project 81837	February 8, 1962 Fig. 3



1. Hydraulic Core: Undrained Steady State Shear Strength, $S_{us} = 700$ psf
2. Dumped Shell: Undrained Steady State Shear Strength, $S_{us} = 2000$ psf
3. Rolled Shell: Drained Strength corresponding to $\phi = 40^\circ$ with no cohesion
4. Glacial Till: Drained Strength corresponding to $\phi = 40^\circ$ with no cohesion

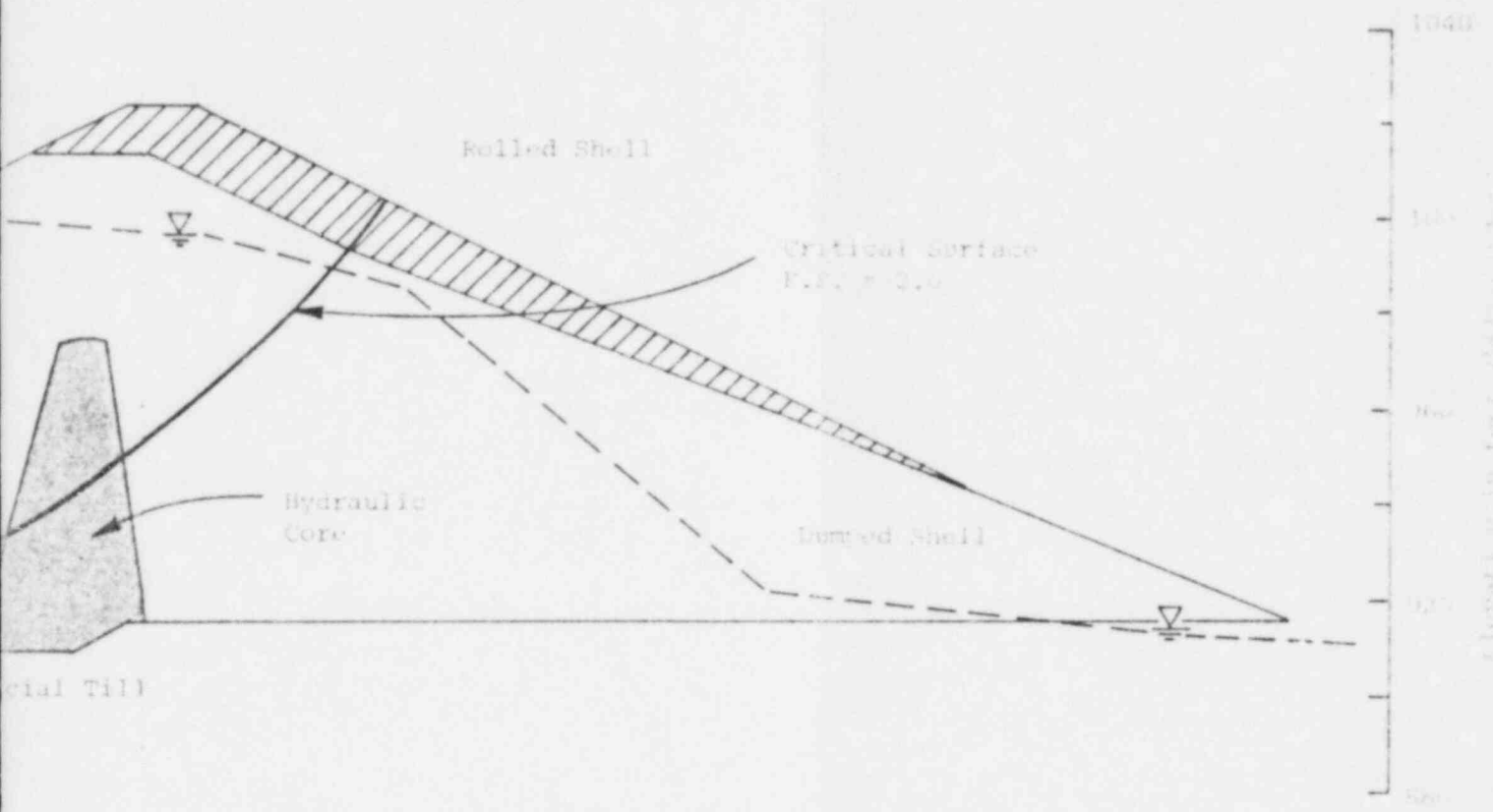



New England Power Company Westborough, Massachusetts	Seismic Stability Evaluation Cherron Dam	SUMMARY OF FLOW SLIDE STABILITY ANALYSIS OF DOWNSTREAM SLOPE
 GEOTECHNICAL ENGINEERS INC. WINCHESTER • MASSACHUSETTS	Project: 1-17	February 3, 1982 Page 4



STRENGTH PARAMETERS USED IN FLOW SLIDE STABILITY ANALYSIS (SEE TEXT FOR DISCUSSION)

1. Hydraulic Core: Undrained Steady State Shear Strength, $S_{us} = 700$ psf
2. Dumped Shell: Undrained Steady State Shear Strength, $S_{us} = 2000$ psf
3. Rolled Shell: Drained Strength corresponding to $\phi = 45^\circ$ with no cohesion
4. Glacial Till: Drained Strength corresponding to $\phi = 40^\circ$ with no cohesion



New England Power Company Westborough, Massachusetts	Seismic Stability Evaluation Sherman Dam	SUMMARY OF FLOW SLIDE STABILITY ANALYSIS OF UPSTREAM SLOPE
 GEOTECHNICAL ENGINEERS INC WINCHESTER • MASSACHUSETTS	Project 51837	February 8, 1992 Fig.

DOCUMENT/ PAGE PULLED

ANO. 8209170055

NO. OF PAGES 2

REASON

PAGE ILLEGIBLE

HARD COPY FILED AT. PDR CF
OTHER _____

BETTER COPY REQUESTED ON _____

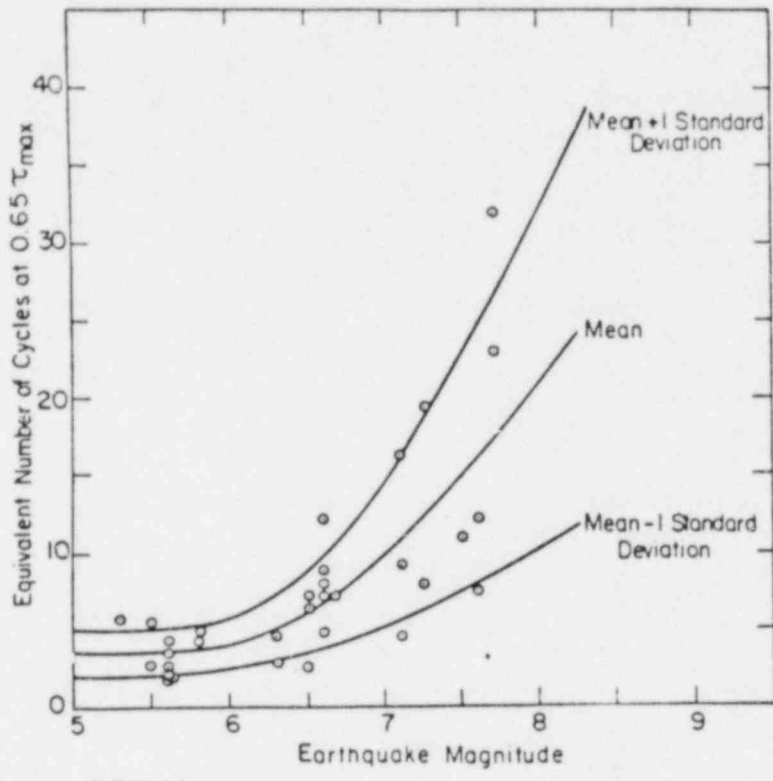
PAGE TOO LARGE TO FILM

HARD COPY FILED AT. PDR CF
OTHER _____


FILMED ON APERTURE CARD NO 8209170055-02

then

8209170055-03



NOTE: Figure adapted from Seed, 1976

New England Power Company Westborough, Massachusetts	Seismic Stability Evaluation Sherman Dam	EQUIVALENT NUMBER OF UNIFORM STRESS CYCLES
 GEOTECHNICAL ENGINEERS INC WINCHESTER • MASSACHUSETTS	Project 81837	February 5, 1982 Fig. 9

DOCUMENT/ PAGE PULLED

ANO. 8209170055

NO. OF PAGES 1

REASON

PAGE ILLEGIBLE.

HARD COPY FILED AT. PDR CF
OTHER _____

BETTER COPY REQUESTED ON _____

PAGE TOO LARGE TO FILM.

HARD COPY FILED AT. PDR CF
OTHER _____

FILMED ON APERTURE CARD NO 8209170055-04

APPENDIX A

SELECTION OF STRENGTH PARAMETERS FOR FLOW SLIDE STABILITY ANALYSES

A1 Hydraulic Core

The range of undrained steady state shear strength, S_{US} , in the hydraulic core of Sherman Dam was estimated from the results of laboratory triaxial tests performed on samples obtained in the field and laboratory studies (GEI, 1982a), as explained in Appendix B.

For an ideal homogeneous soil deposit there is a unique relationship between S_{US} and dry unit weight, termed the steady state line, such that S_{US} increases with increasing density, and for any given dry unit weight there is one value of S_{US} . For most real soil deposits, there is sufficient inhomogeneity that there is a band of steady state lines, as illustrated in Appendix B for the Sherman Dam core, and, consequently, for any given density one would estimate a range of S_{US} .

Based on the band of steady state lines and on the individual, in-situ dry densities (corrected for density changes during sampling and testing, see GEI, 1982a) measured in the tube samples of the core, ranges of S_{US} were estimated and are plotted versus the depths of the tube samples in Fig. A1.

Stability analyses were performed for the three potential slip surfaces illustrated in Fig. A2. From these analyses, the static driving shear stress, τ_d , which could drive a flow slide failure, at points A, B, and C in the core were calculated. These shear stresses were plotted versus depth in Fig. A1 and a relationship between static driving shear stress and depth was constructed.

From Fig. A1, it is seen that in most cases in the core the static driving shear stresses, τ_d , exceed the undrained steady state shear strength, S_{US} . Consequently, it is our opinion that the design earthquake could trigger liquefaction of most of the hydraulic core. For the stability analysis we selected an undrained steady-state shear strength of $S_{US} = 700$ psf. This is approximately a median value of the range of undrained steady-state shear strengths shown in Fig. A1 if the two largest values of S_{US} are excluded. It is reasonable to exclude these two high values because a few isolated pockets of stronger soil will not contribute significantly to the resistance against a flow slide. It should be noted that the plot in Fig. 1 is a semilogarithmic plot and, hence, these two highest S_{US} values are much larger than the other 13 values.

The conclusion that most of the core would liquefy during the design earthquake is supported by the blowcount (Standard Penetration Test) data. In Fig. A3 these data are compared with empirical correlations between blowcounts and earthquake-induced ground failure. The empirical correlations presented in Fig. A3 (Castro, 1975) were developed from data for clean sand deposits beneath level ground which had been subjected to strong-motion earthquakes. For all cases with blowcounts higher than the lines in Fig. A3, ground failure was not observed for that level of earthquake shaking. For cases with blowcounts significantly below the lines, ground failures (liquefaction, excessive settlement, sand boils, etc.) were observed. For blowcounts only slightly below the lines both failure and nonfailure cases were observed. For the Sherman Dam core all of the blowcounts are significantly below the empirical correlation line for the 0.1g maximum ground acceleration. Although the core of the dam is predominantly silty sand and sandy silt (and not clean sand) and the dam is not level ground, so that the correlation does not strictly apply, the low blowcounts do support the conclusion that earthquake-induced liquefaction of the core is likely.

A2 Dumped Shell

In this analysis the term "dumped shell" will refer to both the section of the shell that was dumped in place during construction and the intermediate zone adjacent to the hydraulic core, because samples from both of these zones had similar physical composition and similar blowcounts (GEI, 1982a).

No borings were performed in the upstream shell of Sherman Dam (GEI, 1982a). Hence, no samples of the upstream shell were obtained. Construction records show that the upstream and downstream shells were constructed from the same borrow soils and in the same manner. So, in this analysis, the same stress-deformation properties were assumed for the upstream and the downstream shells of Sherman Dam.

In the borings in the downstream shell, we were not successful in obtaining undisturbed samples, despite ten attempts during the field exploration program (GEI, 1982a). Because of the lack of undisturbed samples, we estimated the stress-deformation properties of the Sherman Dam shell based on comparisons with the Harriman Dam shell.

The visual descriptions, the grain-size distributions, the method of placement and the blowcounts for the Sherman Dam shell are essentially the same as those for the Harriman Dam shell (GEI, 1982a). Therefore, we used results of tests on undisturbed samples of the Harriman Dam shell to estimate the shear strengths of the Sherman Dam shell.

Nine consolidated-undrained triaxial compression (\bar{R}) tests were performed on undisturbed tube samples of the Harriman Dam shell (GEI, 1981b). Steady-state strength data were obtained from five of these tests. However, the void ratios of the specimens as tested were significantly lower than the void ratios of the same samples when removed from the ground. Because the steady-state strength is quite sensitive to void ratio changes, the steady-state strengths measured in the tests had to be corrected for void ratio changes to estimate the steady-state strengths in the field. The correction was based on recent research (GEI, 1982b) which has shown that for several soils with similar but slightly different gradations the steady-state lines are nearly parallel but may be shifted up or down in terms of void ratio. To determine the slope and shape of the steady-state line, \bar{R} tests were performed on compacted specimens of the Harriman Dam shell. To correct the undrained steady-state shear strengths measured in the five \bar{R} tests on undisturbed samples for the measured void ratio changes, we assumed that the steady-state line for each specimen is parallel to the steady-state lines determined from the compacted specimens.

The steady state line from the compacted specimens and the uncorrected and corrected undrained steady-state strengths from the five undisturbed specimens are shown in Fig. A4.

Based on the five corrected strengths from the Harriman Dam shell samples, we selected an undrained steady state shear strength of $S_{us} = 2,000$ psf for the Sherman Dam shell for use in the flow slide analyses. We believe this is a conservative estimate of the strength of the Sherman Dam shell for three reasons. First, the undrained-steady state shear strength is the minimum strength during undrained shear. Second, in the Harriman Dam shell, 93 tube samples were attempted while only 45 samples with greater than 7 in. of recovery were obtained and only 27 of those samples were acceptable for laboratory testing. Hence, the tube samples of Harriman Dam that were tested in the laboratory may represent the looser and less gravelly zones of the shell. Therefore, the average strength of the shell may be higher than that obtained from the tube samples. Third, in the Sherman Dam shell ten tube samples were attempted and no samples with greater than 7 in. of recovery were obtained. This suggests that the Sherman Dam shell may be, on average, denser or more gravelly, and hence stronger, than the Harriman Dam shell.

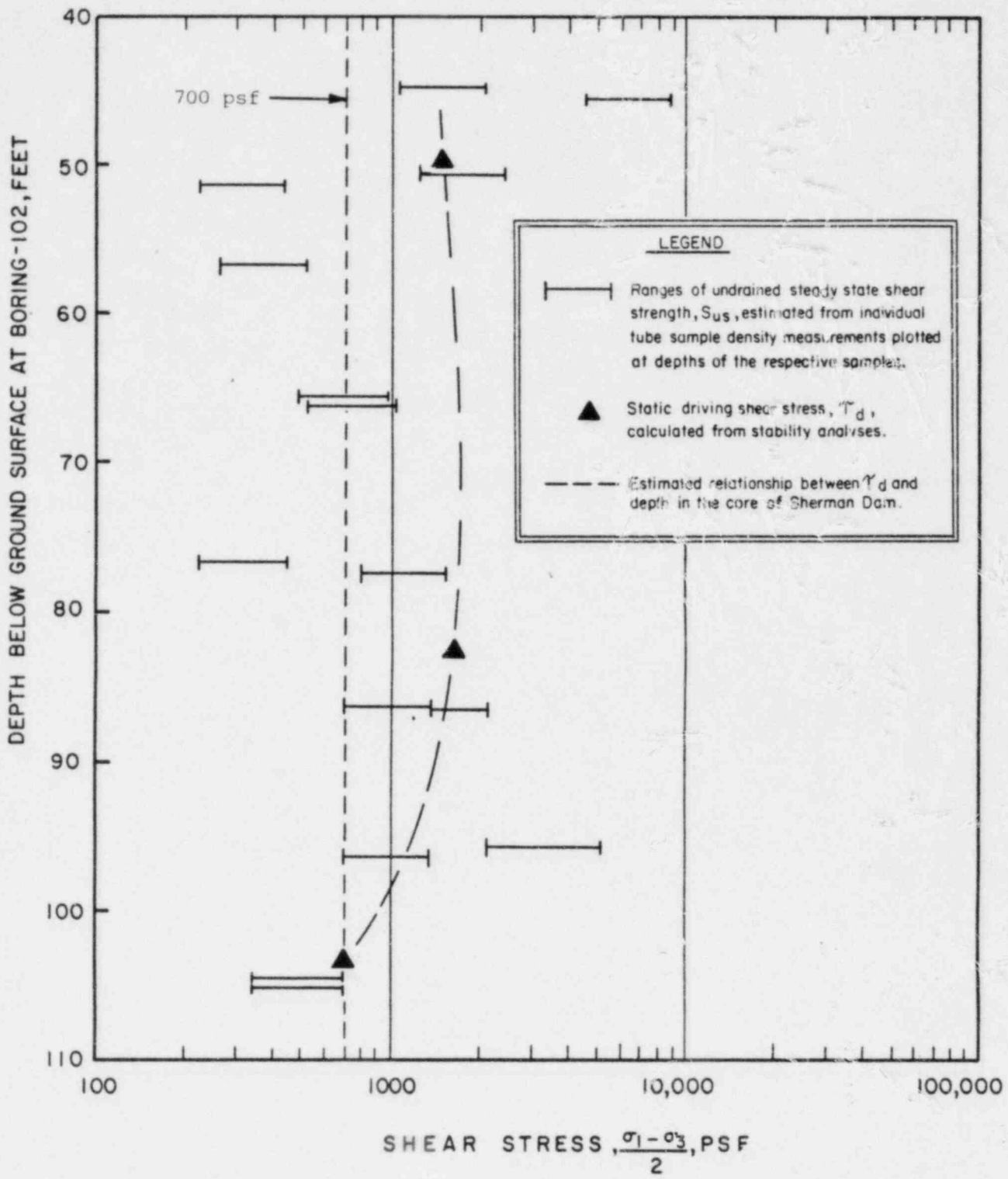
A3 Rolled Shell


The rolled shell in Sherman Dam is above the phreatic surface and a drained strength is appropriate. A friction angle $\phi = 45^\circ$ with zero cohesion was selected based on laboratory tests

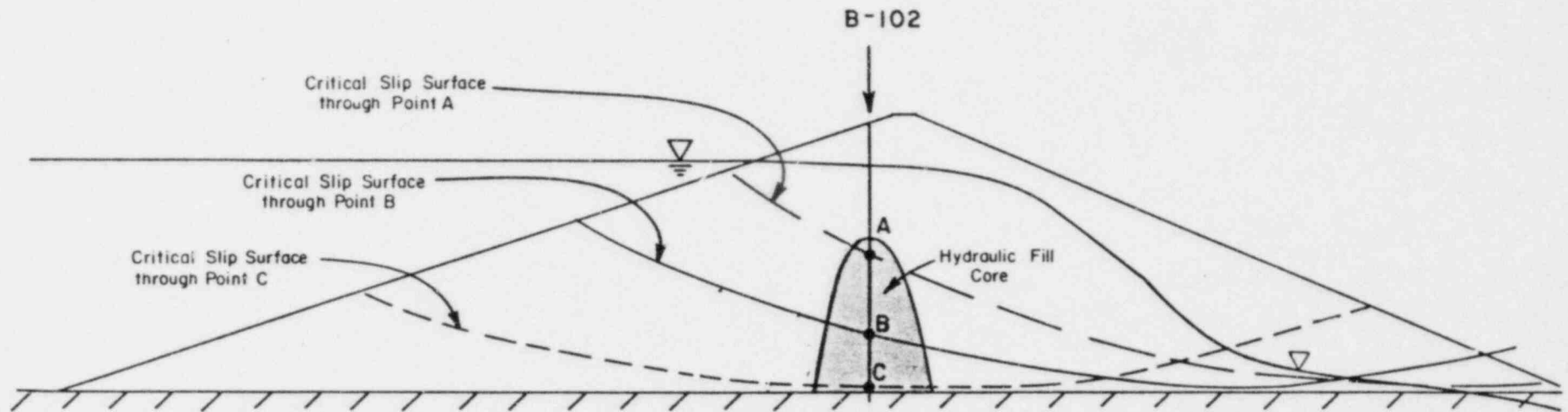
of similar soils from Harriman Dam (GEI, 1981a,b). The high friction angle of this material is attributable to its high density and low confining stress.

A4 Glacial Till Foundation Soil

No strength test data are available for the glacial till foundation soil at Sherman Dam. Based on experience with similar glacial tills we believe that a drained strength with a friction angle $\phi = 40^\circ$ and zero cohesion is a reasonably conservative estimate of the strength of the glacial till beneath the dam. The till is dense enough that it is dilative and, hence, its undrained strength would be greater than its drained strength. However, negative pore water pressures are required to mobilize this higher undrained strength. These negative pressures should not be relied upon in the stability analysis. Therefore, the drained strength, which corresponds to zero induced pore pressure, is a reasonable strength to use in the undrained stability analyses.




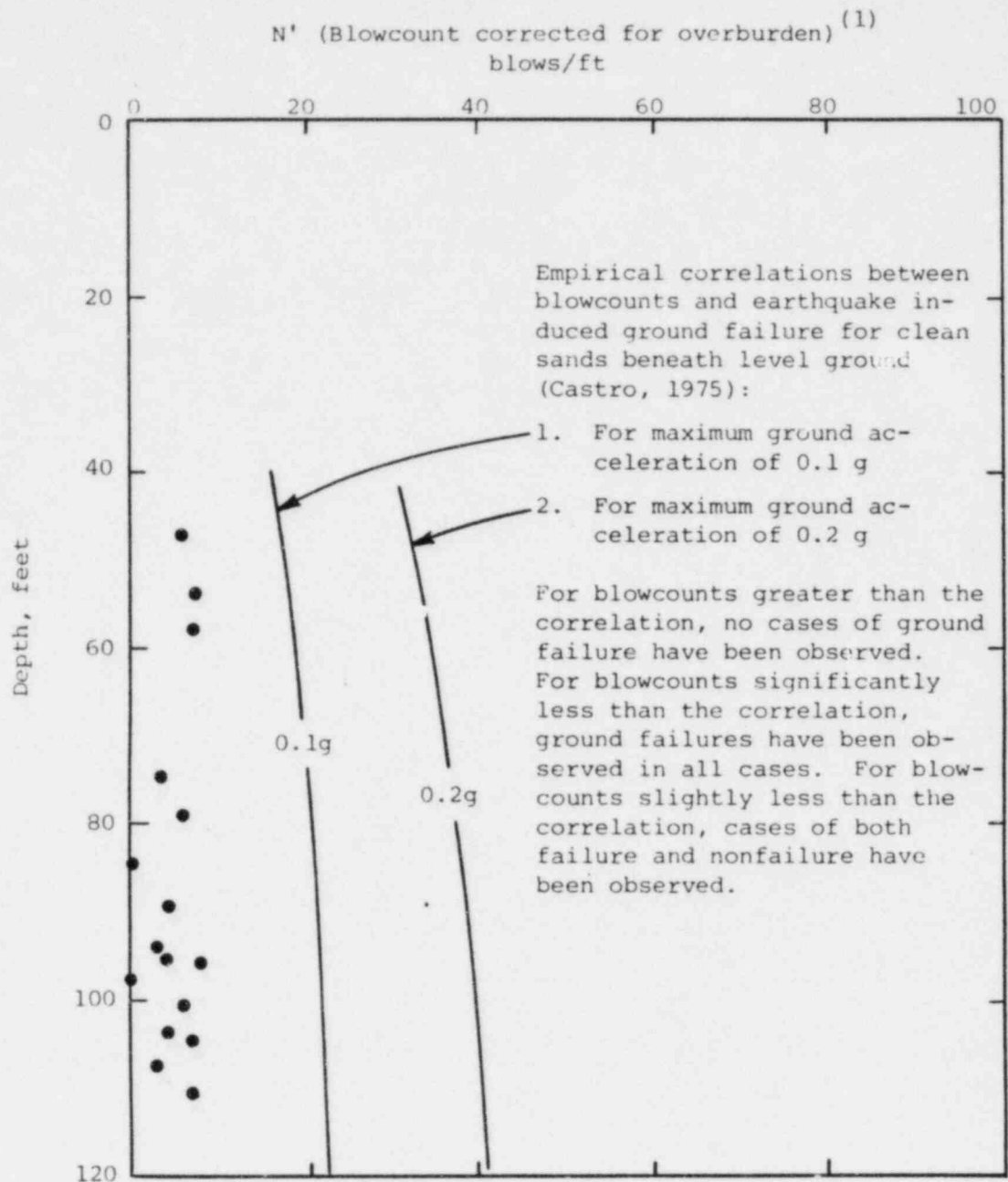
New England Power Company Westborough, Massachusetts	Seismic Stability Evaluation Sherman Dam	IN SITU SHEAR STRESS COMPARED WITH STEADY STATE STRENGTH - CORE MATERIAL
 GEOTECHNICAL ENGINEERS INC WINCHESTER • MASSACHUSETTS		



SHERMAN DAM, CROSS-SECTION
at Station 16 + 00

SCALE 1in. = 60ft.

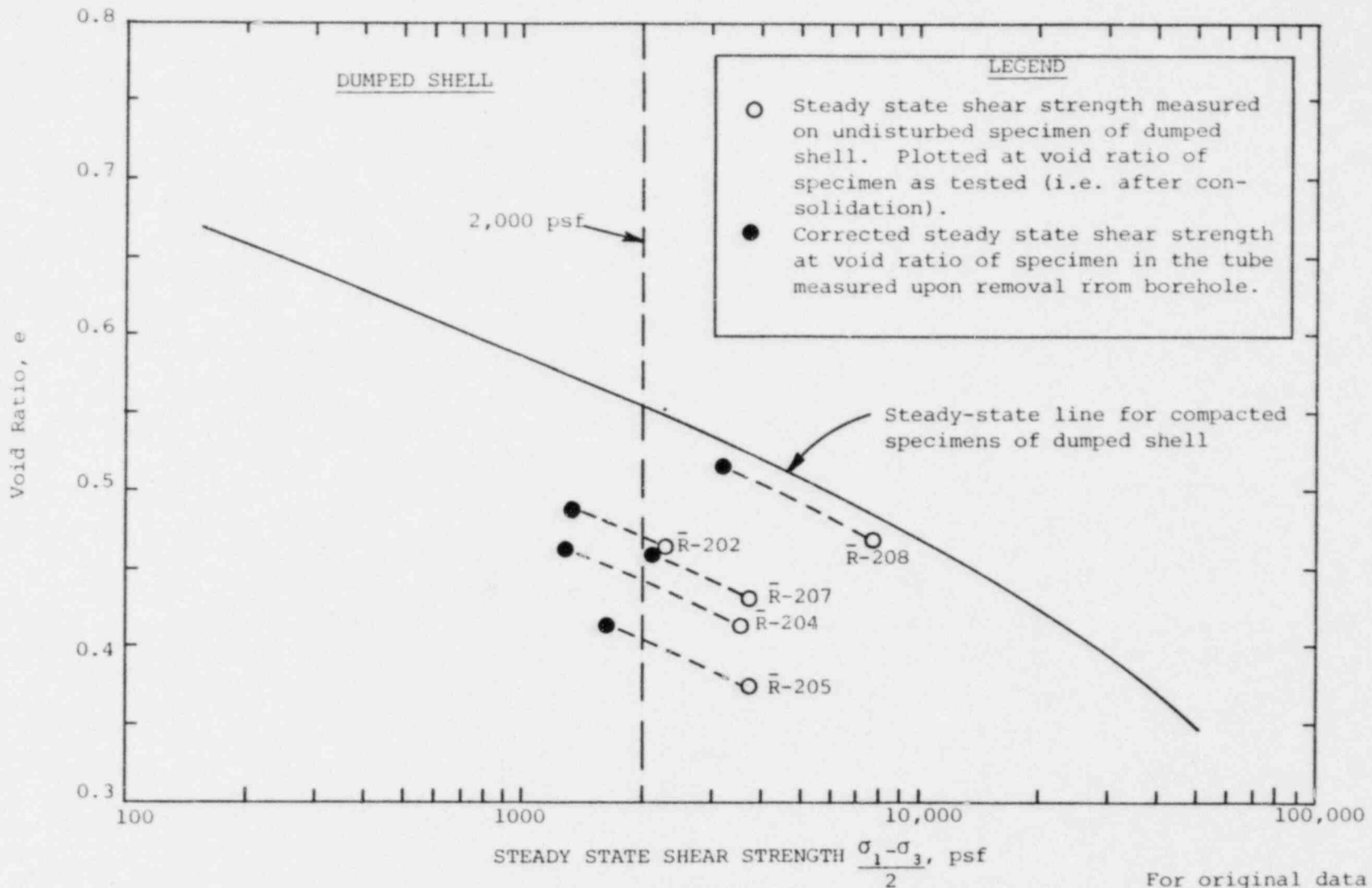
New England Power Company Westborough, Massachusetts	Seismic Stability Evaluation Sherman Dam	STABILITY ANALYSIS ARCS FOR ESTIMATION OF STATIC DRIVING SHEAR STRESSES
 GEOTECHNICAL ENGINEERS INC. WINCHESTER • MASSACHUSETTS	Project 81837	February 5, 1982 Fig. A2




NOTES: (1) $N' = N \left(\frac{50}{\bar{\sigma}_v + 10} \right)$, where $\bar{\sigma}_v$ in psi, N = blowcount for 2-in.-O.D. split-spoon sample.

(2) Data from Borings 102 and 107 in Sherman Dam (GEI, 1982a).

New England Power Company Westborough, Massachusetts	Seismic Stability Evaluation Sherman Dam	COMPARISON OF BLOWCOUNTS AND EARTHQUAKE FAILURE CRITERIA FOR HYDRAULIC CORE
GEOTECHNICAL ENGINEERS INC. WINCHESTER • MASSACHUSETTS	Project 81837	February 5, 1982 Fig. A3



For original data see
GEI 1981b and GEI 1981c

New England Power Company Westborough, Massachusetts	Seismic Stability Evaluation Sherman Dam	STEADY STATE SHEAR STRENGTH DATA FOR DUMPED SHELL FOR HARRIMAN DAM
 GEOTECHNICAL ENGINEERS INC WINCHESTER • MASSACHUSETTS	Project 81837	April 2, 1982 Fig. A4

APPENDIX B

DETERMINATION OF UNDRAINED STEADY STATE SHEAR STRENGTHS FOR HYDRAULIC CORE OF SHERMAN DAM

The following undrained triaxial compression (\bar{R}) tests were performed on samples of the hydraulic core of Sherman Dam:

1. Three tests (\bar{R} -1 through \bar{R} -3) on undisturbed samples consolidated to stresses comparable to the in situ stresses.
2. Six tests (\bar{R} -4 through \bar{R} -6 and \bar{R} -12 through \bar{R} -14) on undisturbed samples consolidated to stresses much higher than the in situ stresses.
3. Five tests (\bar{R} -7 through \bar{R} -11) on specimens compacted from soil taken from the undisturbed samples.

The results of the individual tests have been presented in a previous report (GEI, 1982a).

In the first set of tests (\bar{R} -1 through \bar{R} -3), it was found that when the in situ stresses were reapplied to the specimens, they consolidated to dry unit weights varying from 4 pcf to 7 pcf denser than the in situ densities. The stress-strain curves in these three tests would be described as weakly to moderately dilative. However, because of the density changes, the stress-strain curves and stress paths of these specimens are not representative of the in situ soil, and, in particular, the degree of dilativeness is not representative of in situ conditions.

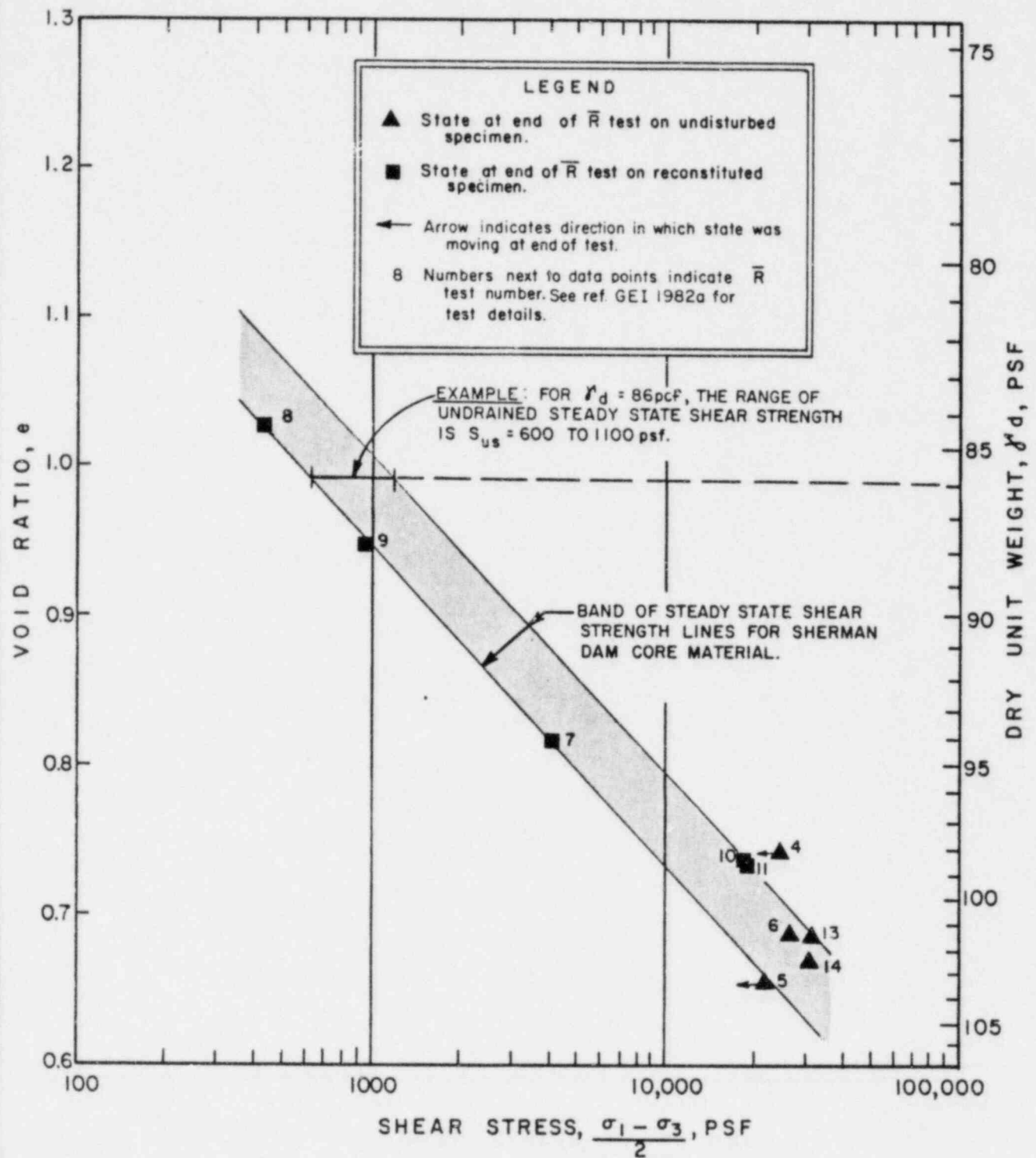
Recent research (GEI, 1982a) has suggested that the most reliable steady-state strength data can be obtained from undrained compression tests on highly contractive specimens. Consequently, to obtain steady-state data from the undisturbed samples, the second set of tests described above was performed at stresses sufficiently high so that the specimens were contractive. The estimated steady-state points are plotted in Figs. B1 and B2 in plots of shear stress (log scale) vs dry unit weight and effective minor principal stress (log scale) vs dry unit weight.

To extend the steady-state data to densities comparable to the field densities, the third set of tests described above was performed on specimens compacted from a batch sample of soil made by mixing similar soils taken from the same tube samples used for the previous \bar{R} -tests, as described in a previous report (GEI,

1982a). These specimens were contractive over a wide range of densities and resulted in the steady-state data shown in Figs. B1 and B2 for reconstituted specimens.

The data from the tests on the undisturbed and reconstituted specimens were combined to develop the bands of steady-state lines shown in Figs. B1 and B2. This interpretation of the data was based on the premise demonstrated in recent research (GEI, 1982b), that, for soils of similar mineralogical composition but with slightly different gradations, the steady state lines will have the same slopes but will vary in their positions in plots such as those in Figs. B1 and B2. The widths of the bands in these figures reflect the inhomogeneity of the hydraulic core.

To estimate the undrained steady state shear strength for a particular sample, Fig. B1 is entered with an estimate of the in situ dry density. For example, if the estimated in situ dry density is 86 pcf, the estimated range of undrained steady state shear strength is $S_{us} = 600$ psf to 1100 psf, as illustrated in Fig. B1.



New England Power Company
Westborough, Massachusetts

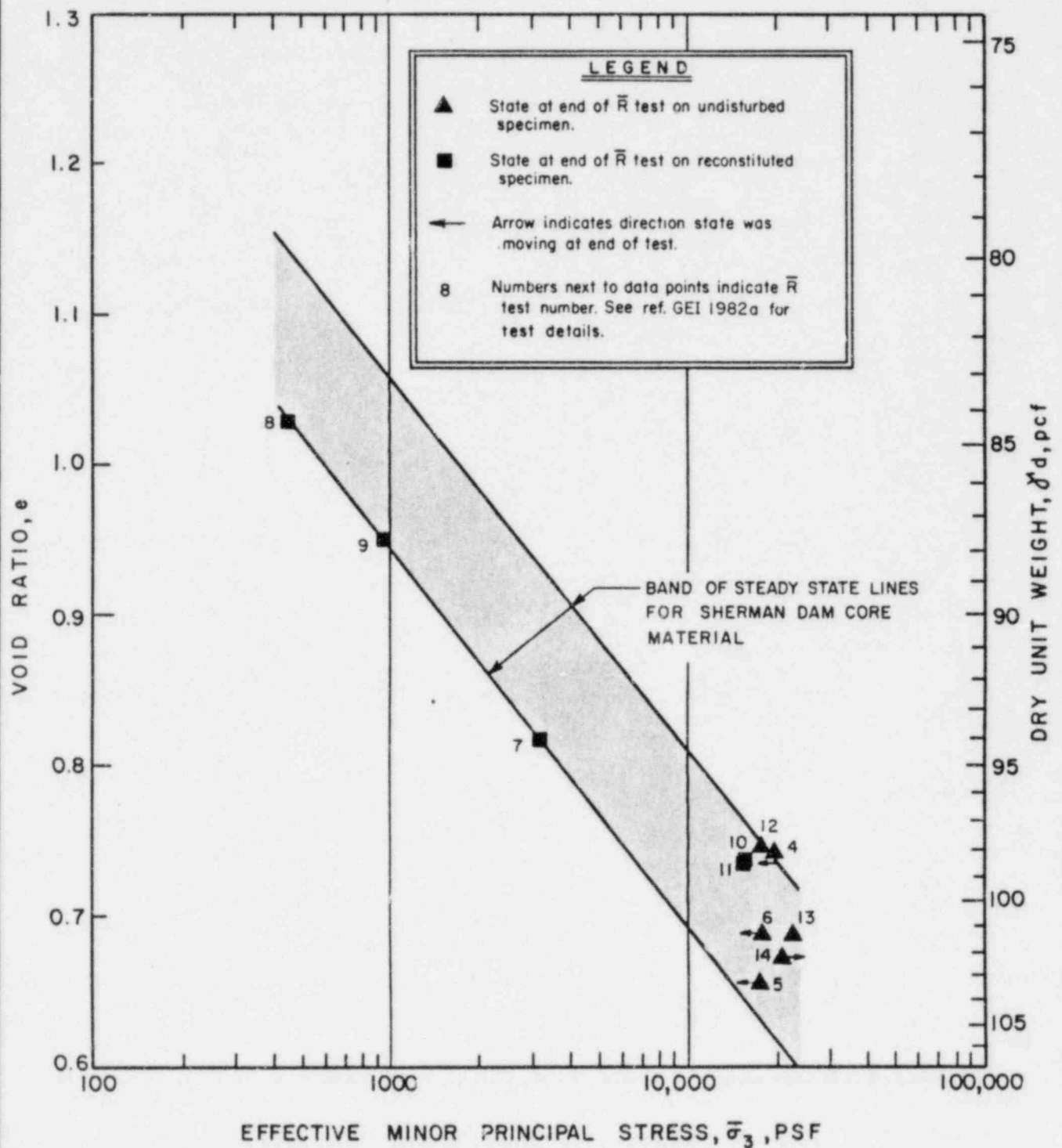
Seismic Stability
Evaluation
Sherman Dam

STEADY STATE SHEAR
STRENGTH LINES -
CORE MATERIAL

 **GEOTECHNICAL ENGINEERS INC.**
WINCHESTER • MASSACHUSETTS

Project 81837

February 5, 1982 Fig. B1



New England Power Company
Westborough, Massachusetts

Seismic Stability
Evaluation
Sherman Dam

STEADY STATE LINES
CORE MATERIAL



GEOTECHNICAL ENGINEERS INC
WINCHESTER • MASSACHUSETTS

Project 81837

February 5, 1982

Fig. B2

APPENDIX C

SOME DETAILS OF THE EVALUATION OF STRAINS AND DEFORMATIONS DURING SEISMIC LOADING

C1 General

This appendix contains discussions of some of the details of four items referred to in Section 5 of the text, namely:

1. Selection of dynamic soil properties
2. Accumulated strain data
3. Stress redistribution due to computed strain incompatibility
4. Sensitivity analyses

C2 Selection of Dynamic Soil Properties

For input to the two-dimensional finite-element program (FLUSH), dynamic soil properties, consisting of an initial value of shear modulus, an initial value of damping and variations of these properties with shear strain, must be selected for each finite element in the mesh.

Because no dynamic soil property data are available for Sherman Dam, the dynamic properties selected for the shell and the core were based on the results of resonant column and small-strain cyclic triaxial tests on undisturbed specimens from Harriman Dam, which were presented in GEI (1981a). The dynamic soil properties measured in tests on the Harriman Dam shell were used directly for the Sherman shell because of the inferred similarity in stress-deformation properties of the two materials based on similarities in physical composition, method of placement, and in blowcounts (GEI 1982a). The dynamic soil properties measured in tests on specimens from the core of Harriman Dam were corrected for use in this analysis, to account for the lower densities measured in the core of Sherman Dam. The corrections were made according to relationships presented in Hardin and Richart (1963) and Kim and Novak (1981).

C3 Accumulated Strain Data

Relationships between accumulated strain after seven cycles of load and cyclic stress ratio were developed from the results of laboratory cyclic load tests on undisturbed samples. The cyclic stress ratio is defined as $\tau_{fy}/\bar{\sigma}_{fc}$, where τ_{fy} is the

cyclic shear stress on the potential failure plane and $\bar{\sigma}_{fc}$ is the effective normal consolidation stress on the same plane.

Cyclic test results from nine cyclic triaxial (CR) tests on anisotropically consolidated ($K_C = \bar{\sigma}_{1c}/\bar{\sigma}_{3c} = 2.0$) undisturbed specimens from the dumped shell of Harriman Dam were used to evaluate strains accumulated in the shell of Sherman Dam during earthquake loading. The data were plotted in GEI (1981b) in terms of $\tau_{fy}/\bar{\sigma}_{fc}$ vs accumulated shear strain after seven cycles, and this plot is reproduced herein as Fig. C1.

Cyclic test data from five anisotropically consolidated ($K_C = 2.0$) and two isotropically consolidated ($K_C = 1.0$) specimens from the core of Sherman Dam were used to evaluate the accumulated shear strains in the hydraulic core. The cyclic triaxial test results are plotted in Fig. C2 in terms of cyclic stress ratio $\tau_{fy}/\bar{\sigma}_{fc}$ vs accumulated shear strain after seven cycles.

Although the test results showed that the cyclic resistances of the anisotropically consolidated specimens of the Sherman Dam core were generally greater than the cyclic resistances of isotropically consolidated specimens, and that the cyclic resistance generally decreased with increasing minor effective consolidation stress, the variations due to these factors appear to be less than that due to inhomogeneities among the different samples. Consequently, different relationships for different minor effective consolidation stresses (as used for the shell) could not be developed for the core. Instead, the curve plotted in Fig. C2, which represents a conservative bound to all of the test data from the Sherman Dam core, was used to calculate the accumulated shear strains in the core.

C4 Stress Redistribution due to Computed Strain Incompatibility

As stated in Section 5.4 of the text, in some cases the large differences between the deformabilities of the hydraulic core and of the dumped shell lead to incompatibility in the computed strains at the boundaries of the two zones, when the computed strains are determined directly from Figs. C1 and C2 and the earthquake shear stresses calculated in the finite element analysis. The following hand-calculation procedure was used to estimate compatible strains due to redistribution of shear stresses from the more deformable core to the less deformable shell.

At a given depth in the hydraulic core the earthquake shear stress ratio, $\tau_{avg}/\bar{\sigma}_v$, was computed based on the results of the finite-element analysis. From the curve plotted in Fig. C2, the accumulated shear strain corresponding to the computed normalized

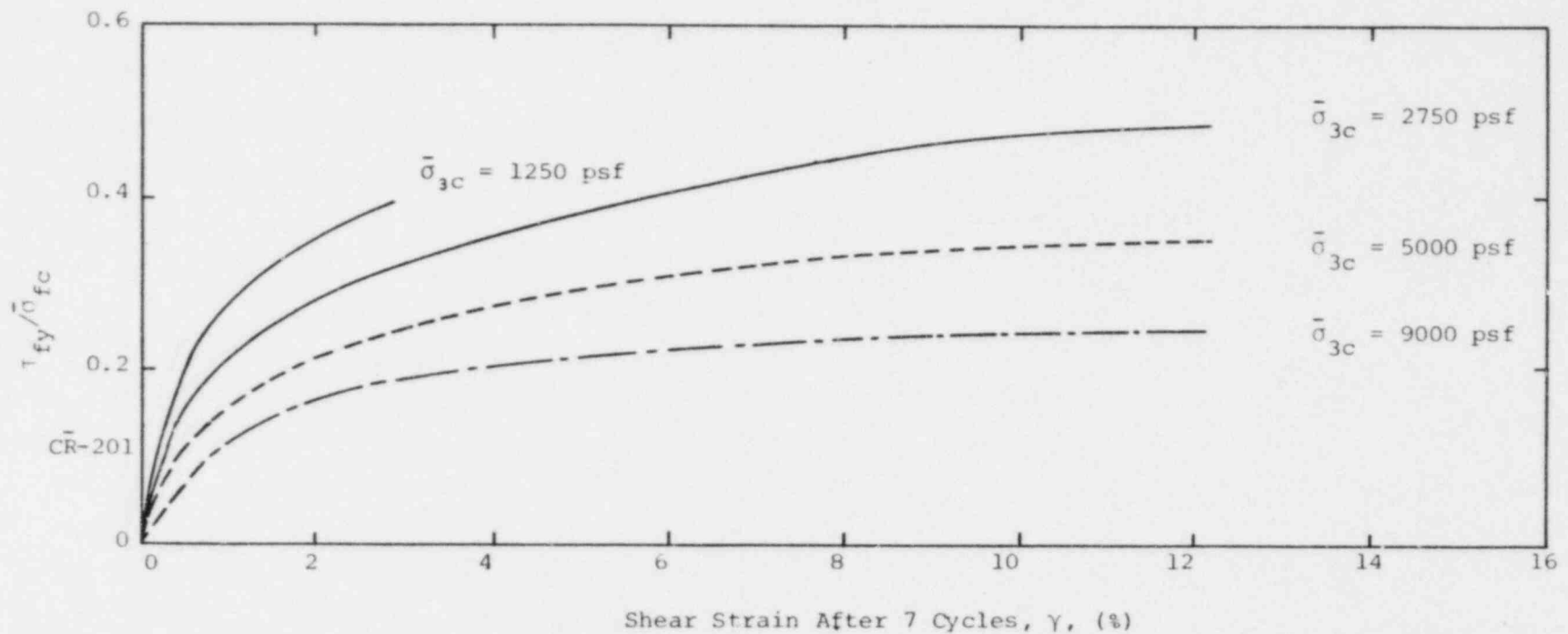
earthquake shear stress was determined by equating $\tau_{fy}/\bar{\sigma}_v = \tau_{avg}/\bar{\sigma}_v$. Similarly, the accumulated shear strain in the shell, at the same depth, immediately adjacent to the core, was determined from the earthquake shear stress calculated in the finite element analysis and from Fig. C1. If the accumulated strain in the shell was less than in the core, shear stress was subtracted from the core and added to the shell, and the accumulated strains redetermined from Figs. C1 and C2. Using this method the strain in the core was decreased and the strain in the shell was increased until the accumulated strains calculated for the core and for the shell adjacent to the core were equal and therefore compatible.

C5 Sensitivity Analyses

Analyses were performed to evaluate the sensitivity of the finite-element analysis to variations in (1) the modulus of the core and (2) the size of the core.

According to the relationships presented by Hardin and Richart, 1963, and Kim and Novak, 1981, the moduli determined from tests on the Harriman Dam core should be multiplied by about 0.65 to correct for the lower densities in the Sherman Dam core. To evaluate the sensitivity of the analysis to this correction factor, analyses were performed with Sherman Dam core moduli equal to 0.50 times and 1.00 times the values measured on the Harriman Dam core samples. Both analyses were performed with the Housner earthquake record scaled to a maximum ground acceleration of 0.1g. As shown in Fig. C3, this variation in core modulus had no significant effect on the calculated earthquake shear stresses. The other analyses presented in this report were performed with a core modulus of 0.65 times that determined from the Harriman Dam core samples.

Sensitivity analyses were also performed to evaluate the effect of core size. Three sizes, small, medium, and large, as shown in Fig. C4, were considered. We believe these three sizes cover the reasonable range of expected core size, based on the borings and on the construction records. The analyses for all three sizes were performed with the Housner earthquake record scaled to a maximum ground surface acceleration of 0.1g. As can be seen in Fig. C4, there is some variation of earthquake shear stress with changes in core size. However, the variations are not large enough to significantly affect the final calculated deformations. Therefore, the other analyses presented in this report were performed with the medium size core, which is our best estimate of the actual core configuration.



- NOTES: (1) Plot taken from Fig. 8, GEI (1981b).
 (2) Curves are from test results performed on samples from the dumped shell of Harriman Dam. Test results were corrected for change in void ratio during specimen handling and consolidation, and for loss of "aging effects" during sampling. See GEI (1981b) for details.
 (3) Dashed curves extrapolated from measured data.
 (4) All tests performed on specimens with consolidation ratio $K_c = 2.0$.

New England Power Company
 Westborough, Massachusetts

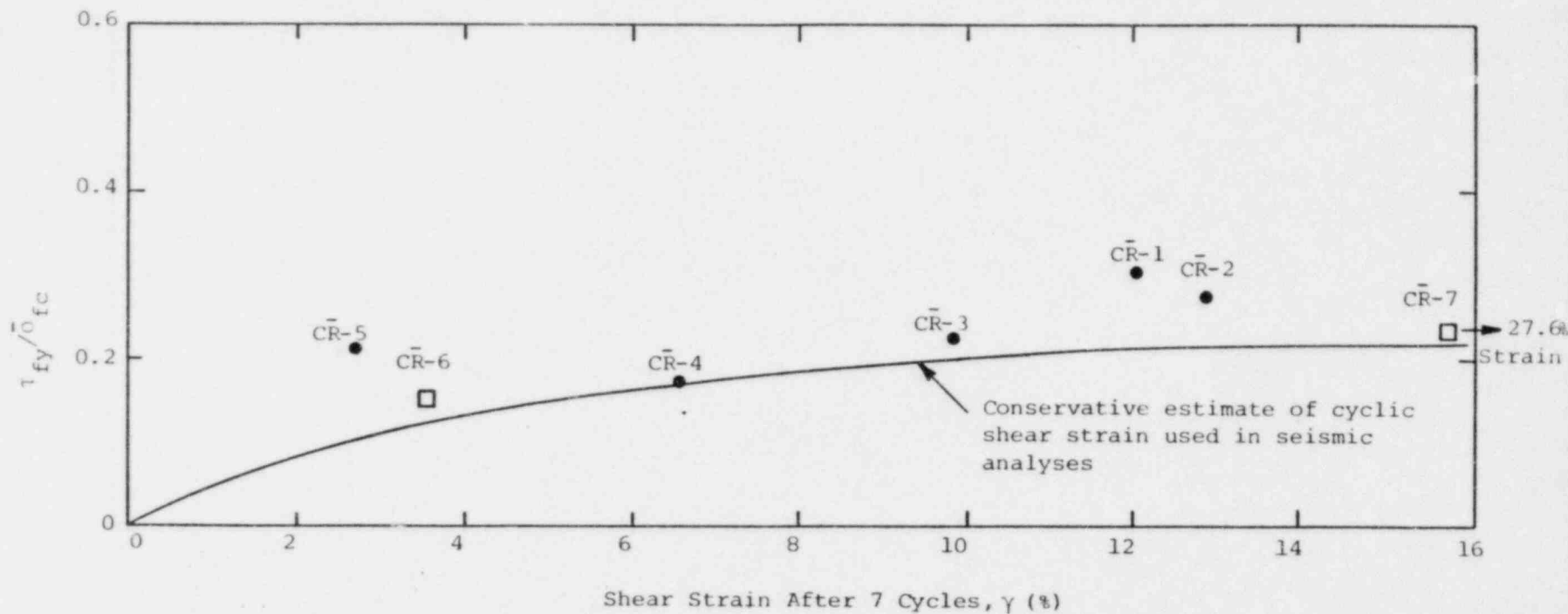
Φ GEOTECHNICAL ENGINEERS INC.
 WINCHESTER • MASSACHUSETTS

Seismic Stability
 Evaluation
 Sherman Dam

Project 81837

CYCLIC SHEAR STRESS
 VS ACCUMULATED SHEAR
 STRAIN - DUMPED SHELL

February 8, 1982 Fig. C1



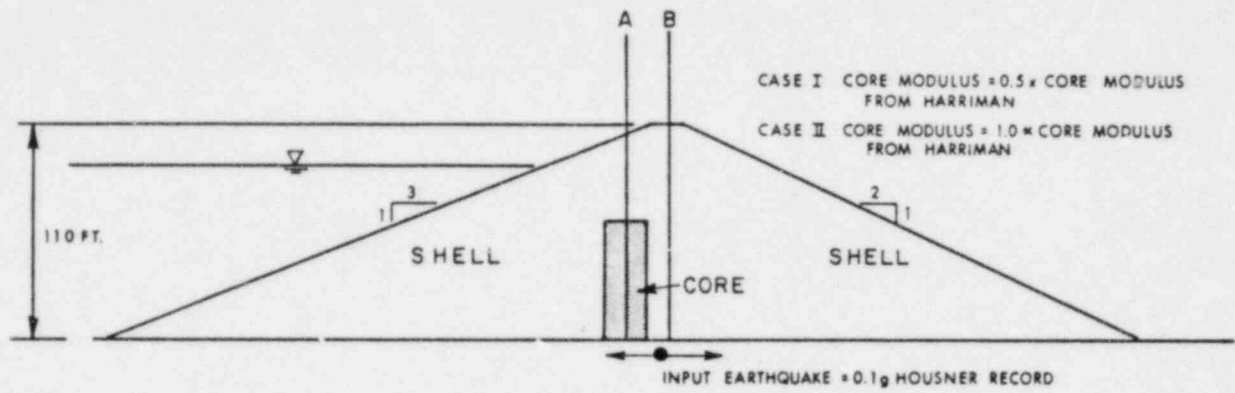
NOTE: See reference GEI (1982a) for details of CR tests.

LEGEND

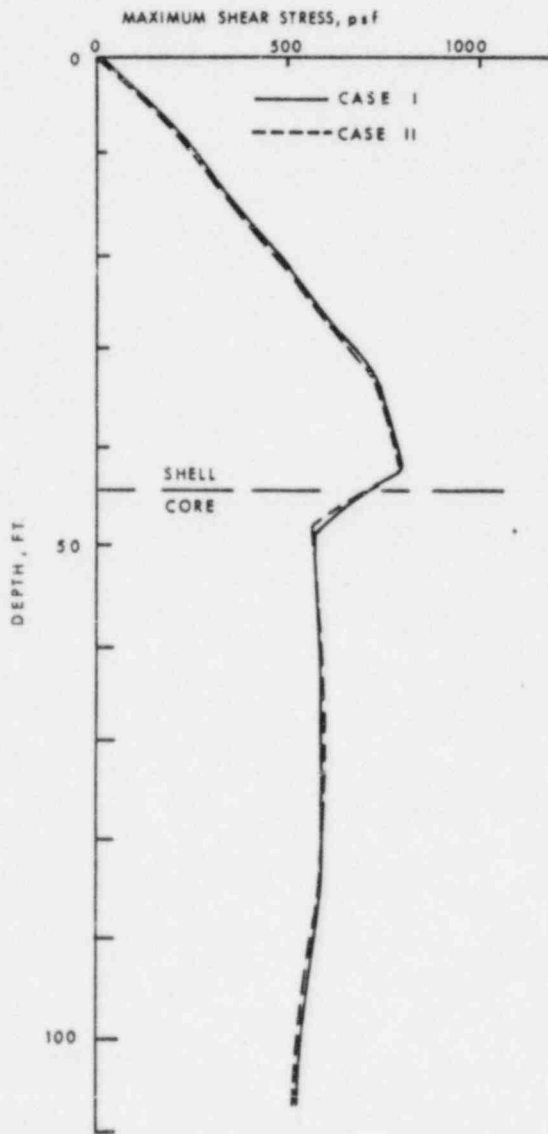
● CR test result for anisotropically consolidated ($K_c = 2.0$) undisturbed specimen

□ CR test result for isotropically consolidated ($K_c = 1.0$) undisturbed specimen

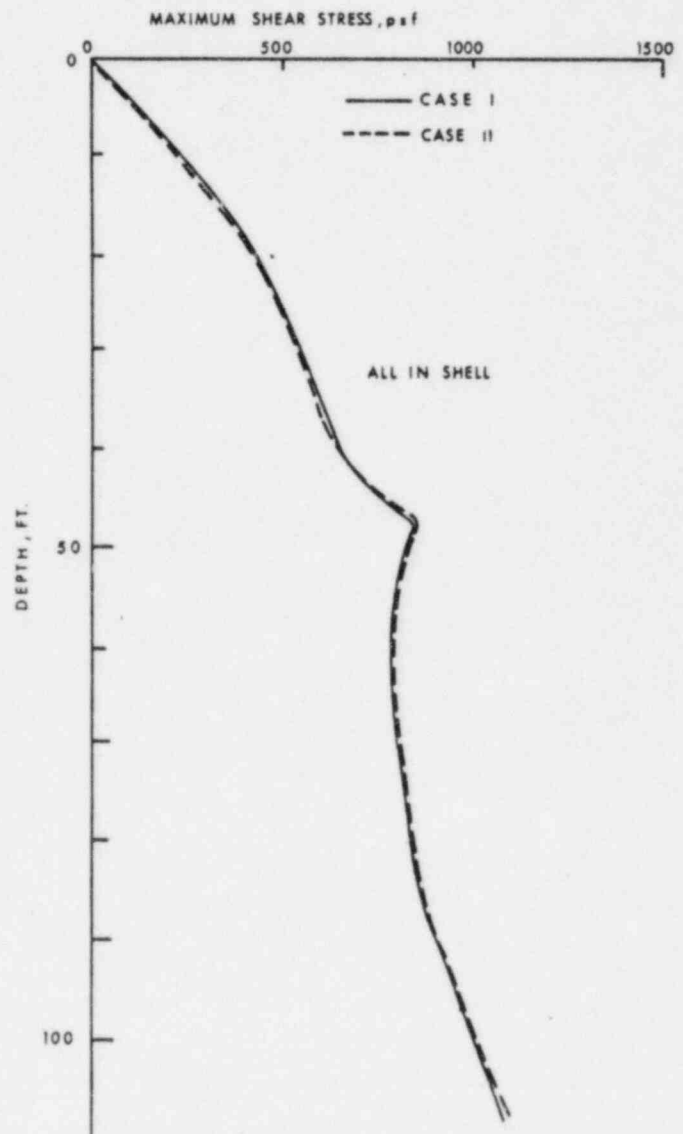
New England Power Company Westborough, Massachusetts	Seismic Stability Evaluation Sherman Dam	CYCLIC SHEAR STRESS VS ACCUMULATED SHEAR STRAIN HYDRAULIC CORE
Φ GEOTECHNICAL ENGINEERS INC WINCHESTER • MASSACHUSETTS	Project 81837	February 5, 1982 Fig. C2



a) DAM SECTION ANALYZED



b) SHEAR STRESS vs. DEPTH, SECTION A



c) SHEAR STRESS vs. DEPTH, SECTION B

New England Power Company
 Westborough, Massachusetts



GEOTECHNICAL ENGINEERS INC.
 WINCHESTER • MASSACHUSETTS

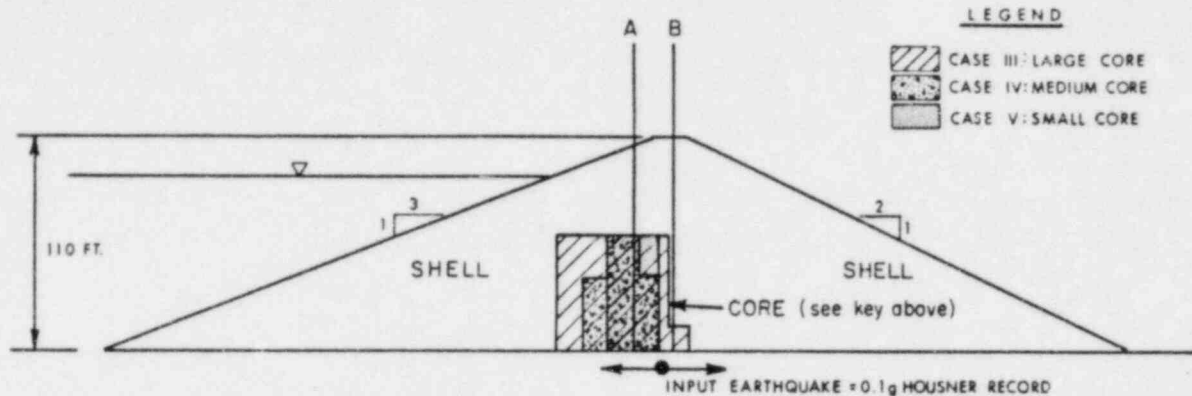
Seismic Stability
 Evaluation
 Sherman Dam

Project 81837

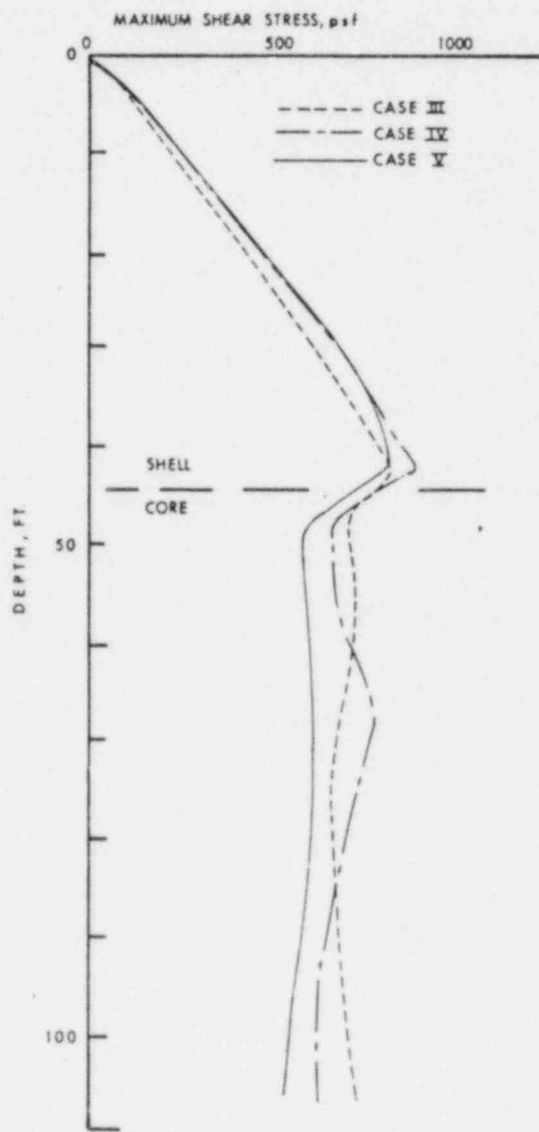
EFFECT OF VARIATION OF
 CORE MODULUS ON RESULTS
 OF FINITE ELEMENT ANALYSIS

April 2, 1982

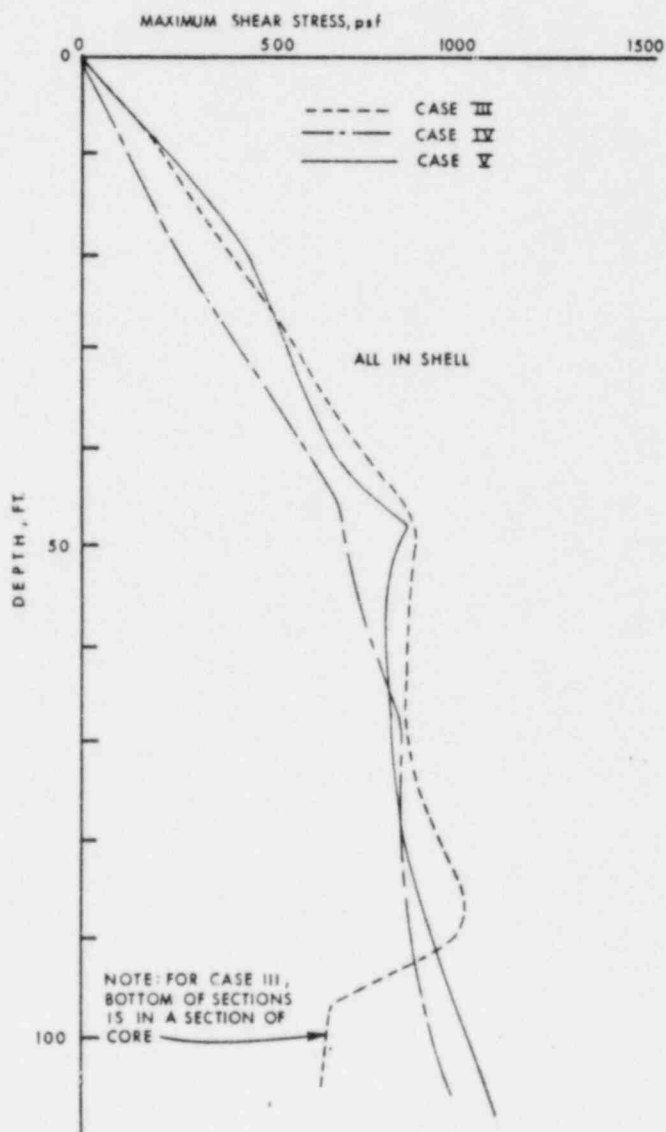
Fig. C3



a) DAM SECTION ANALYZED and PROPERTIES USED



b) SHEAR STRESS vs. DEPTH, SECTION A



c) SHEAR STRESS vs. DEPTH, SECTION B

New England Power Company
Westborough, Massachusetts

Seismic Stability
Evaluation
Sherman Dam

EFFECT OF VARIATION OF
CORE SIZE ON RESULTS OF
FINITE ELEMENT ANALYSIS



GEOTECHNICAL ENGINEERS INC
WINCHESTER • MASSACHUSETTS

Project 81837

April 2, 1982

Fig. C4